AMERICAN OPTIONS PRICING USING HJM APPROACH

by

Wedige Sandesh Kushantha Fernando

A dissertation submitted to the faculty of
The University of North Carolina at Charlotte
in partial fulfillment of the requirements
for the degree of Doctor of Philosophy in
Applied Mathematics

Charlotte

2017

Approved by:

Dr. Mingxin Xu

Dr. Jaya Bishwal

Dr. Oleg Safronov

Dr. Weidong Tian

©2017
Wedige Sandesh Kushantha Fernando
ALL RIGHTS RESERVED

ABSTRACT

WEDIGE SANDESH KUSHANTHA FERNANDO. American Options Pricing Using HJM Approach.(Under the direction of Dr. Mingxin Xu)

With the development of financial markets and increasing demand for managing risk exposure, researchers and practitioners have developed various financial instruments over the years. Options, Futures, Forwards, Swaps are few examples of such instruments. There are many financial models design to price such derivatives and they all have one thing in common: arbitrage free valuation of these derivative contracts.

In this thesis we focus on pricing mechanism of one the widely traded derivatives: American option. We employ HJM forward modeling approach introduced by Heath, Jarrow and Morton (1992). HJM model is originally introduced as an alternative method to bond pricing. Traditional bond pricing is done via short rate modeling while HJM method attempt to price bonds via modeling the evolution of entire yield curve.

In recent years, Schweizer and Wissel (2008) and Carmona and Nadtochiy (2009) extend the forward modeling idea to equity market by modeling forward volatility allowing researchers to look at a dynamic curve which relax the Black-Scholes constrain of constant volatility. This modeling paradigm also allows easy calibration to market data, which makes the HJM model popular among practitioners. Here we propose an alternative approach to value American type options in the spirit of HJM approach. Since American option is essentially an optimal stopping problem, it's value given by the Snell envelop of the value process. By adapting HJM method method using forward drift we formulate a new value process of American option. We propose a new value function, a new stopping criteria and a new stopping time. We investigate this new method in both additive and multiplicative model settings using the forward modeling approach. Then we give an example for the new proposed method under

additive model to solve American option pricing problem theoretically.

Numerical investigation of the additive and multiplicative models is carried out for Option Matrix data for August 2007 to August 2015 using three methods: principal component analysis, robust principal component analysis and Karhunen- Loeve transformation.

Contents

List of Figures

List of Tables

CHAPTER 1: INTRODUCTION TO HJM APPROACH FOR FIXED INCOME AND EQUITY MARKET

Assume that we are interested in finding the fair value of contingent claim V_t. Arbitrage free price under the risk neutral measure is given by $V_t = E[e^{-\int_0^t r_u du} G(t)|F_t]$ where r_u is the interest rate and $G(t)$ is the payoff of the claim. Goal of this thesis is to use forward rate approach to find arbitrage free price of American options under forward modeling. As a pretext, we first discuss the fixed income market and then the equity market in the spirit of HJM forward modeling methodology.

1.1 Fixed income market

The fixed income security is generally known as an investment that provides periodic income to the investor at predefined intervals. Bonds, Swaps, Caps, Floors, Swaptions are few examples of fixed income instruments. The key risk of fixed income market is the interest rate risk. Therefore, ability to model and capture the movement of interest rate is very important in fixed income instruments pricing.

1.1.1 Short rate

Short rate r_t is a realization from yield curve such that interest rate applicable for infintely small maturity time. Short rate is fundamental to interest rate modeling since many fixed income market instruments have been based on the dynamics of the short rate. Typically short rate dynamics is given by the following stochastic

differential equation

$$dr_t = a(t,T)dt + b(t,T)dW_t \tag{1.1}$$

Where $a(t,T)$, $b(t,T)$ are coefficient of the drift and the volatility respectively. Despite their shortcomings and limitations that we will discuss later, short rate models are still used in practice and remain popular mainly because of their easy implementation and existence of closed form solution for many liquid assets. There are several commonly used short rate models: Merton model, Vasicek model, CIR model, Hull and White model, Ho - Lee model.

1.1.2 Bond

Definition: A T- maturity zero coupon bond (pure discount bond) is a contract that guarantees it's holder the payment of one unit of currency at time T, with no immediate payments. Contract value at time $t < T$ is denoted by $B(t,T)$. Clearly $B(T,T) = 1$.

Bond price is usually done through modeling the interest dynamics. The most common choice is the short rate model. Let us illustrate how bond pricing is done via one of the common short rate models: Vasicek model.

1.1.3 Vasicek model

On the probability space (Ω, F, P), equipped with filtration F_t, the risk neutral pricing formula for bond price is given by

$$B(t,T) = E\left[e^{-\int_t^T r_u du} B(T,T) \,|\, F_t\right] = E\left[e^{-\int_t^T r_u du} \,|\, F_t\right].$$

It is important to note that discounted bond price is a martingale under the risk neutral measure, hence assuring the price $B(t,T)$ is arbitrage free. Recall that under Vasicek (1977), the model dynamics is given by

$$dr_t = a(b - r_t)dt + \sigma dW_t. \tag{1.2}$$

Vasicek is an example of Ornstein-Uhlenbeck (O-U) processes with a constant volatility σ. Solving this equation we get:

$$r_t = e^{-bt}r_0 + (1 - e^{-bt})\frac{a}{b} + \int_0^t e^{-b(t-u)}du \tag{1.3}$$

Using the fact that $\int_t^T r_u du$ is Gaussian, hence calculating it's expected value and variance we are able to represent the bond price as:

$$B(t,T) = e^{A(T-t)+C(T-t)r_0} \tag{1.4}$$

Where $A(T-t) = \frac{4ab-3\sigma^2}{4b^2} + \frac{\sigma^2-2ab}{2b^2}(T-t) + \frac{\sigma^2-ab}{b^3}e^{-b(T-t)} - \frac{\sigma^2}{4b^3}e^{-2b(T-t)}$ and $C(T-t) = -\frac{1}{b}(1 - e^{-b(T-t)})$. Vasicek (1977)

1.1.4 Yield Curve

Yield curve is a graph which depicts the average rate of return implied by bonds over time. This curve is also known as term structure of interest rate. Let $t \geq 0$. Let $T_1, T_2....T_n$ be the maturities. Let $Y(t, T_i)$ where $i = 1, 2, 3....n$. Then yield curve is given by $T \to Y(t,T)$. In general, yield curve can take many shapes, most common one is being upward slope with higher rates for higher maturities. Although inverted yield curve is also theoretically possible and have occurred practically in the past. Denote $\hat{B}(0, T_i)$ as the market prices for zero coupon bonds with different maturities $T_1, T_2...T_n$. The yield curve $T \to Y(0,T)$ can be calculated as

$$Y(0,T_i) = \frac{1}{T_i}\ln\frac{\hat{B}(T_i,T_i)}{\hat{B}(0,T_i)} \quad \Leftrightarrow \quad \hat{B}(0,T_i) = \hat{B}(T_i,T_i)e^{-T_iY(0,T_i)}$$

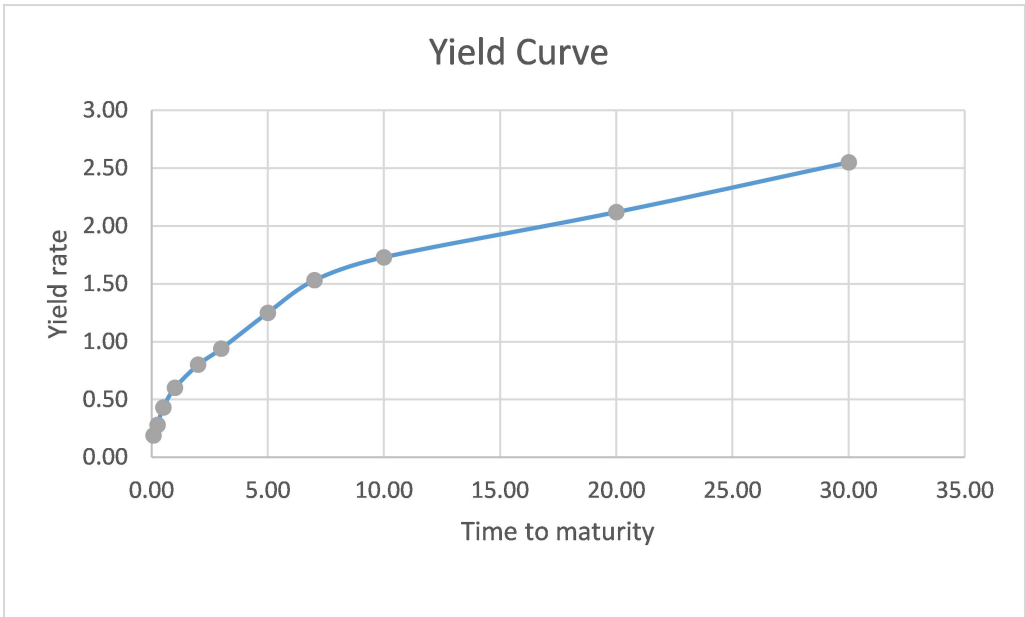

Figure 1.1: Yield Curve

Where $\hat{B}(T_i, T_i) = 1$.

The yield $Y(0, T)$ over time period $[0, T]$ is known as the long rate. The yield curve created for U.S treasures rates for February 13, 2017 is given in following graph.

1.2 Calibration issues of short rate approach

whenever the functions $A(T, t)$ and $C(T, t)$ are calculable, bond price can be evaluated by closed form solution given by the equation (1.2). Vasicek model belongs to a general class of interest rate models known as affine models. Advantage of such models is that they are easy to calibrate. This is usually done by fitting the model parameters a, b, σ to the actual market data. This process is known as the calibration. As mentioned earlier, in order to tune the Vasicek bond price to market data, we need

to estimate a, b, σ. Theoretically, this would only require bond prices for three different maturities T_1, T_2, T_3 from the market. But the issue is, bond prices calculated using such a model tend to deviate vastly from the actual observed bond prices. In other words, term structure implied by this model is different from the actual market evolution. As a fix, we may employ frequent calibration but then the pricing model becomes many frequently re-calibrated single period models rather than single, dynamic model over the maturity of the instruments we intend to price. As Carmona (2009) pointed out, frequency of re-calibration and when it is optimal to re-calibrate needs to be addressed. In a nutshell, short rate does not provide a clear picture of forward evolution the interest rate dynamics. This highlights the need of having a dynamic dynamic model which is consistent with market data.

Heath, Jarrow and Morton (1992) proposed a method to solve above mentioned shortcomings. They addressed the issues of calibration of short rate models and be consistent with market instruments through so called forward modeling approach. This method tries to model the dynamics of $f_t(T)$ is given by $df_t(T) = \alpha_t(T)dt + \beta_t(T)dW_t$. Using market bond prices $\hat{B}(t,T)$, forward rate is given by the following equation.

$$f_t(T) = -\frac{\partial}{\partial T} \ln \hat{B}(t,T) \tag{1.5}$$

Note that from equation (1.5) and initial bond price $\hat{B}(0,T)$ observed at time $t = 0$, we can calculate the initial forward rate curve

$$f_0(T) = -\frac{\partial}{\partial T} \ln \hat{B}(0,T) \tag{1.6}$$

Dynamics of the forward rate is given by

$$f_t(T) = f_0(T) + \int_0^t \alpha_u(T)du + \int_0^t \sigma_u(T)dW_u \tag{1.7}$$

Calibration under forward rate approach only require knowing the initial forward curve $f(0,T)$ as it is considered as an input to the evolution of forward curve given by $f_t(T)$. There is no need of frequent re-calibration.

One of the key components in forward modeling approach is given by it's spot consistency condition. Spot consistency condition under forward interest rate modeling is given by $f_t(t) = r_t$. In other words, spot consistency condition tells us that instantaneous forward rate is equal to the short rate at t. Another important aspect of the forward modeling approach is no arbitrage drift condition. Heath-Jarrow-Morton (1992) showed that this model achieve no arbitrage by imposing restrictions on the model drift $\alpha_t(T)$. This condition is given by $\alpha_t(T) = \beta_t(T) \int_t^T \beta_t(u)du$.

1.3 HJM Forward modeling approach and it's importance

We discussed the short rate approach and it's limitations until now. Here we will present the differences of two modeling paradigms. For any given time t, short rate models represent a single value in it's state space, r_t. Forward rate at time t, model represent an entire evolution of term structure of interest rate or it's distribution. Carmona (2009). This allows HJM approach to price forward starting financial instruments as well.

Another difference of two models can be seen in their bond pricing equations. Under the risk neutral measure, bond price $B(t,T)$ using short rate is given by

$$B(t,T) = E[e^{-\int_t^T r_u du} \mid F_t]. \tag{1.8}$$

According to Heath, Jarrow and Morton (1992), same bond price is given by

$$B(t,T) = e^{-\int_t^T f_t(u)du} \tag{1.9}$$

We can noticed that under the short rate approach, it requires to simulate r_t, then take a risk neutral expectation to calculate the bond price. Once the HJM models is implemented, it is more convenient to price financial instruments because HJM method does not require to take risk neutral expectation. Forward rate, $f_t(u)$ is directly observed from the forward rate curve.

1.4 Equity market

The equity market consists of stocks and it's associated derivative products which are traded through exchanges or over the counter. The key risk component in equity market is the volatility of the underlying stock. It is well known that the Black - Scholes formula provides a closed form solution for European type derivatives. For stock price dynamics given by $ds_t = rS_t dt + \sigma S_t dW_t$, interest rate r and constant volatility σ, European call option price can be calculated by

$$V_t = E[e^{-r(T-t)}(S_T - K)^+ | F_t] \tag{1.10}$$

Where K is the strike price. Price of the call option is explicitly given by Black - Scholes formula as follows

$$V(t,T) = BS(S_t, T, t, K, r, \sigma) = S_t N(d_1) - K e^{r(T-t)} N(d_2) \tag{1.11}$$

Where $d_1 = \dfrac{\ln(\frac{S_t}{K}) + (r + \frac{\sigma^2}{2})(T-t)}{\sigma\sqrt{T-t}}$ and $d_2 = d_1 - \sigma\sqrt{T-t}$.

Black - Scholes model still serves as the backbone for options pricing although model operates under some strong assumptions. These assumptions seems to contradict actual market observations. Constant volatility assumption is one of them. Upon this realization, researchers and practitioners focused on more realistic volatility models that resonate the actual market volatility. These models treat volatility

as a stochastic process and not a constant anymore.

1.5 Implied Volatility and forward implied volatility

Definition: Implied volatility $\hat{\sigma}_t$ of an option is implicitly defined as the parameter $\hat{\sigma}_t$ that yields the actual observed option price when it is substituted into the Black-Scholes formula. i.e $BS(S_t, T, t, \hat{\sigma}_t, K, r) = \hat{V}(t, T)$, where $\hat{V}(t, T)$ option prices observed from the market.
When the option prices are observed in market place, by inverting Black-Scholes formula, we may calculate implied volatility.

Then we can construct the implied volatility curve using observed $\hat{\sigma}$. But historical evidence suggests that the derivative price, $\hat{V}(t, T)$ varies with K and T contrary to the Black-Scholes assumptions. This result in a frequent mismatch between Black-Scholes implied volatility model and actual volatility implied by the market data. Therefore, frequent re-calibration of the model is needed.

In order to address calibration issue faced by the implied volatility surface, Schweizer and Wiessel (2008) proposed forward implied volatility modeling in the spirit of HJM methodology. They denoted the forward implied volatility as

$$X(t, T) = \frac{\partial}{\partial T}((T - t)\hat{\sigma}_t^2(T)) \tag{1.12}$$

Which follows,

$$\hat{\sigma}_t^2(T) = \frac{1}{T - t}\int_t^T X(t, u)du \tag{1.13}$$

Also the dynamics of $X(t,T)$ is given by

$$dX_t(u) = \alpha_t(u)dt + \beta_t(u)dW_t \tag{1.14}$$

Calibration carried out for forward implied volatility by replacing σ by $\sigma_t(T)$ in Black-Scholes model. For an example, calibrated call option price is given by

$$C_t^T = BS(S_t, T, t, \sqrt{\frac{1}{T-t}\int_t^T X(t,S)dS}, K, r) \tag{1.15}$$

Calibration is not an issue since $X(0,T)$ is an input forward volatility curve. Therefore this is an improvement of traditional implied volatility model. No arbitrage for the model is achieved by imposed conditions on $\alpha_t(u)$ and it is given in proposition 2.2 of Schweizer and Wiessel (2008). Another key feature of forward modeling philosophy is the spot consistency condition. Spot consistency condition for forward local volatility id given by $X(t,t) = \sigma_t$.

Let's turn our attention to the local volatility model.

1.6 Local volatility and forward local volatility

Consider the governing equation

$$dS_t = r_t S_t dt + \sigma(t, S_t)S_t dW_t \tag{1.16}$$

The diffusion coefficient defined as $\sigma_t = \sigma(t, S_t)$ is known as local volatility. This makes In other words, the local volatility is a function of t and S_t. Note that randomness is caused by S_t in the local volatility model. Therefore it is easy to calibrate to local volatility model than to implied volatility model.

Local volatility can also be viewed as the current expected variance of τ and K where $\tau = T - t$, T is the maturity and K is the strike price. Considering the fact that local

volatility can be expressed as a function of τ and K, Dupire (1994) defined the local volatility as

$$\sigma_t(\tau, K)^2 = \frac{2\partial_\tau C_t(\tau, K)}{K^2 \partial^2_{KK} C_t(\tau, K)} \tag{1.17}$$

Note that $C_t(\tau, K)$ is the call option price on S_t. Advantage of the local volatility model is that calibration is not an issue since we can observe $\sigma_0(T, K)$ as $\hat{C}_0(T, K)$ available in the market for any trading day.

Using the Dupire local volatility function defined in equation (1.17), Carmona and Nadtochiy (2009) modeled the forward local volatility as

$$d\sigma_t(\tau, K) = \alpha_t(\tau, K)dt + \beta_t(\tau, K)dW_t \tag{1.18}$$

Where $\tau = T - t$. No arbitrage condition imposed on $\tilde{\alpha}_t$ and the spot consistency condition for the forward local volatility model is given by theorem 4.1 of Carmona and Nadtochiy (2009).

CHAPTER 2: FORWARD MODELING APPROACH

We reviewed the bond pricing and it's HJM modeling approach by identifying forward interest rate is the key. This was stated in sections $1.1 - 1.3$ of chapter 1. In sections $1.4 - 1.6$, we reviewed the importance of forward volatility modeling as the key to European options pricing in the equity market. In this chapter, we will discuss American option pricing in the spirit of HJM forward modeling approach.

American Option is a financial derivative which allows the option holder to exercise the option at any time during it's lifetime.

For risk free interest rate $r > 0$, the value of the American option with payoff G_t is given by

$$V_0 = \sup_{0 \leq \tau \leq T} E[e^{r\tau} G_\tau]$$

where τ is a stopping time. Note that this is an optimal stopping problem. As we stated, our goal is to solve the optimal stopping problem in HJM setting. We will identify forward drift modeling is the key in to solve the problem. We will provide an alternative value function to traditional value function. Then we will give a new stopping criteria and a new stopping time to this new approach. Further we provide spot consistency condition, no arbitrage drift condition for our model using HJM philosophy. Finally we will discuss calibration. We carry out our analysis under two models: additive model and multiplicative model.

2.1 Optimal stopping problem under traditional approach

In this section, we will introduce the optimal stopping problem. Let (Ω, F, P) be the probability space equipped with complete and right continuous filtration F_t. Let G_t be the gain process adapted to the filtration F_t and

$$E(\sup_{0\leq t\leq T}|G_t|) < \infty \tag{2.19}$$

When $r = 0$, main optimal stopping problem for the gain process G_t is given by

$$V_0 = \sup_{0\leq\tau\leq T} E[G_\tau] \tag{2.20}$$

where τ is the stopping time. Since $T < \infty$ this is a finite time horizon optimal stopping problem.

Solution to the above problem is given by the Snell envelop or essential supremum of G_t. It is defined by

$$V_t = \operatorname*{ess\,sup}_{t\leq\tau\leq T} E[G_\tau|F_t] \tag{2.21}$$

with the optimal stopping time τ^* is defined by

$$\tau_t^* = \inf\{t \leq s \leq T : V_s = G_s\} \tag{2.22}$$

For the sake of simplicity, we denote τ_t^* by τ^* from now on.

2.2 Additive model for forward modeling

We are trying to solve the above optimal stopping problem in HJM setting. As a motivation, let's recall forward modeling in fixed income and equity market. Forward interest rate is the key in bond pricing. Similarly, forward volatility modeling is the key in the equity market. We state that forward drift is the key in American option pricing. Therefore, we will attempt to solve the above problem in an alternative approach using forward modeling of the drift.

2.2.1 Motivation for forward drift

Assume the dynamics of G_t is given by

$$dG_t = \mu_t dt + \sigma_t dW_t \tag{2.23}$$

where

$$\int_t^T |\mu_u| du < \infty \quad P.a.s. \tag{2.24}$$

and

$$\int_t^T \sigma_u^2 du < \infty \quad P.a.s \tag{2.25}$$

Since τ^* is the optimal stopping time, τ^* defined in (2.22) is optimal. From the definition of Snell envelop (2.21) we have $V_t = E[G_{\tau^*}|F_t]$.

Therefore, consider $V_t = E[G_{\tau^*}|F_t]$. Notice that,

$$\begin{aligned} E[G_{\tau^*}|F_t] &= G_t + E[\int_t^{\tau^*} (\mu_u du + \sigma_u dW_u)|F_t] \\ &= G_t + E[\int_t^{\tau^*} \mu_u du|F_t] + E[\int_t^{\tau^*} \sigma_u dW_u|F_t] \end{aligned}$$

But $\int_t^{\tau^*} \sigma_u dW_u$ is a martingale. So $E[\int_t^{\tau^*} \sigma_u dW_u | F_t] = 0$. This implies $V_t = G_t + E[\int_t^T \mu_u 1_{\{\tau^* \geq u\}} du | F_t]$. By Fubini theorem,

$$V_t = G_t + \int_t^T E[\mu_u 1_{\{\tau^* \geq u\}} du | F_t] \tag{2.26}$$

We can see that the volatility of the gain process does not contribute to the value function. In other words, only the drift of the gain process matters for modeling V_t.

2.2.2 HJM approach to American option pricing under additive model

Let V_t be the price of American option with payoff G_t. For the sake of simplicity, we let $r = 0$ to demonstrate the forward drift. For $r > 0$ refer to the example given in section 2.5.

For American option price V_t and the gain process G_t we define the forward rate

$$f_t(T) = \frac{\partial}{\partial T}(V_t - G_t) \tag{2.27}$$

Assume the dynamics of the forward drift process, $f_t(u)$ is given by the diffusion process

$$df_t(u) = \alpha_t(u)dt + \beta_t(u)dW_t \tag{2.28}$$

Where

$$\int_t^T |\alpha_t(u)| du < \infty \quad \text{a.e. P} \tag{2.29}$$

$$\int_t^T \beta_t^2(u) du < \infty \quad \text{a.e. P} \tag{2.30}$$

We define the forward drift to satisfy (2.27). Therefore,

$$f_t(u) = E[\mu_u 1_{\{\tau^* \geq u\}} | F_t] \tag{2.31}$$

By the forward drift $f_t(u)$ defined in equation (2.27) and comparing it to the equation (2.26) we get (2.31) under the assumption (2.23) and $r = 0$.

2.2.3 Spot consistency condition

Let us introduce one of the integral part of HJM modeling philosophy known as the spot consistency condition. Recall that in bond pricing, spot constancy condition explains the instantaneous forward rate. This is equal to short rate r_t given at time t. In the forward implied volatility model, spot consistency condition tells us that spot forward implied volatility $X(t,t)$ equal to σ_t. Where σ_t is the instantaneous volatility of the gain process. Similarly, we will identify a different spot consistency condition for American option. This new spot consistency condition tell us that instantaneous forward drift is equal to μ_t. This is one of the key features in our model.

Theorem 1. *Let the dynamics of $f_t(u)$ be given by* (2.28) *under the conditions* (2.29) *and* (2.30). *Define the spot consistency condition of forward drift model as $f_t(t) = \lim_{T \to t} f_t(T)$. Then $f_t(t) = \mu_t$.*

Proof. Recall that $f_t(u) = E[\mu_u 1_{\{\tau^* \geq u\}} | F_t]$.

Therefore,

$f_t(t) = \lim_{T \to t} f_t(T) = \lim_{T \to t} E[\mu_T 1_{\{\tau^* \geq T\}} | F_t]$. But by dominated convergence theorem,

$f_t(t) = E[\lim_{T \to t} \mu_T 1_{\{\tau^* \geq T\}} | F_t] = \mu_t$. This completes the proof. □

Therefore we affirm that spot consistency condition for American option pricing under the additive forward drift model is given by μ_t. Which is the drift of the gain process.

2.2.4 Stopping time

So far we have proposed a new model to solve the optimal stopping problem and associated spot consistency condition. We will address the new stopping time for the additive model in this subsection.

Let's recall familiar stopping time under the traditional model as in equation (2.22)

$$\tau^* = \inf\{t \leq s \leq \tau : G_s = V_s\}$$

According to (2.27), the value function is given by

$$V_s = G_s + \int_s^T f_s(u)du$$

Since the value function $V_s \geq G_s$ in continuation region, we can conclude that $\int_s^T f_s(u)du \geq 0$. Therefore, we observe that optimal time to stop the value process is when $\int_s^T f_s(u)du \leq 0$. In other words, the optimal stopping time for the value process under the additive model is

$$\tau^* = \inf\{t \leq s \leq \tau : \int_s^T f_s(u)du \leq 0\} \tag{2.32}$$

2.2.5 No arbitrage drift condition

Let's recall that model must be inherently arbitrage free under the HJM philosophy because there is no risk neutral expectation of the payoff. Heath-Jarrow-Morton(1992) proved that no arbitrage can be achieved by imposing conditions on the drift of the forward rate. Following theorem states the no arbitrage theorem for the additive model.

Theorem 2. *Let dynamics of G_t given by* (2.23) *under the conditions* (2.24) *and* (2.25)*. Let dynamics of $f_t(u)$ be given by* (2.28) *under the conditions* (2.29) *and* (2.30) *is given by $\alpha_t(T) = 0$ a.e on $[0, \tau^*]$. In our model given in* (2.27)*, V_t is*

is modeled by the drift of the gain process. But under the traditional approach, it requires a conditional expectation to model the value function. This is the difference in modeling aspect of out model and the traditional value process.

Proof.

$$
\begin{aligned}
V(t) &= G_t + \int_t^T f_t(u)du \\
dV(t) &= dG_t + d(\int_t^T f_t(u)du) \\
&= \mu_t dt + \sigma_t dW_t + \int_t^T df_t(u)du - f(t,t)\frac{\partial t}{\partial t}dt \\
&= \mu_t dt + \sigma_t dW_t - f(t,t)dt + (\int_t^T \alpha_t(u)du)dt + (\int_t^T \beta_t(u)du)dW_t
\end{aligned}
$$

Note that $f(t,t) = \mu_t$ by spot consistency condition. Therefore

$$dV_t = (\textstyle\int_t^T \alpha_t(u)du)dt + (\int_t^T \beta_t(u)du + \sigma_t)dW_t.$$

Recall that $V(t,T)$ is a martingale in continuation region.
Therefore $\int_t^T \alpha_t(u)du = 0$ for $0 \leq t \leq \tau^*$. By differentiating above integral with respect to T we have $\alpha_t(T) = 0$ a.e on $[0, \tau^*]$.
This completes the proof.

□

We have proposed a new value function to American option problem, it's spot consistency condition, a new stopping criteria and a new stopping time. This completes the theoretical discussion about additive model. We will present the multiplicative counterpart of forward modeling approach in the next section.

2.3 Multiplicative model

In this section, we will propose multiplicative type model for value function V_t to solve the optimal stopping problem.

Let's recall from equations (2.21) and (2.22) the traditional value process of optimal stopping process and it's optimal stopping time when $r = 0$. When for $r > 0$, same value process is given by

$$V_t = \operatorname*{ess\,sup}_{t \le \tau \le T} E[e^{-r(\tau - t)} G_\tau | F_t]$$

$$\tau^* = \inf \{t \le s \le T : V_s = G_s\}$$

Let the dynamics of G_t be given by

$$dG_t = \mu_t G_t dt + \sigma_t G_t dW_t \tag{2.33}$$

where the dynamics of dG_t satisfies the conditions (2.24) and (2.25). Note that unlike in equation (2.23), G_t is an exponential now. Note that equation (2.29) implies,

$$G_t = G_0 e^{\int_0^t (\mu_u - \frac{1}{2}\sigma_u^2) du + \int_0^t \sigma_u dW_u} \tag{2.34}$$

2.3.1 HJM approach for American option pricing under multiplicative model

Recall that forward drift under the additive model is given by (2.17). We define the multiplicative counterpart of the additive model as

$$f_t(T) = \frac{\partial}{\partial T} ln \frac{V_t}{G_t} \tag{2.35}$$

Where the dynamics of $f_t(u)$ is given by (2.28) under the conditions (2.29) and (2.30) and the dynamics of G_t is given by (2.33) under the conditions (2.24) and

(2.25).

According to the equation (2.35) the value function of the American option is given by

$$V_t = G_t e^{\int_t^T f_t(u)du}$$

Again under the multiplicative model, we model V_t using the drift while under the traditional model V_t requires a conditional expectation.

2.3.2 Spot consistency condition

We will present the corresponding spot consistency condition for multiplicative model in the following theorem.

Theorem 3. *Let the value process V_t be given by* (2.35) *and the dynamics of G_t be given by* (2.33) *under the conditions* (2.24) *and* (2.25). *Let the dynamics of $f_t(u)$ be given by* (2.28) *under the conditions* (2.29) *and* (2.30). *Define the spot consistency condition as $f_t(t) = \lim_{T\to t} f_t(T)$. Then $f_t(t) = \mu_t - r - \frac{1}{2}\sigma^2$ a.e on $[0, \tau^*]$. Where r is the risk free interest rate.*

Proof. Note that $f_t(T) = \frac{\partial}{\partial T} ln \frac{V_t}{G_t}$. This implies
$f_t(T) = \lim_{h\to 0} \frac{1}{h}(ln \frac{V_t(T+h)}{G_t} - ln \frac{V_t(T)}{G_t})$. This is equivalent to
$f_t(T) = \lim_{h\to 0} \frac{1}{h} ln \frac{V_t(T+h)}{V_t(t)}$.
$f_t(t) = \lim_{T\to t} f_t(T) = \lim_{T\to t} \lim_{h\to 0} \frac{1}{h} ln \frac{V_t(T+h)}{V_t(t)}$
Hence
$f_t(t) = \lim_{h\to 0} \frac{1}{h} ln \frac{V_t(t+h)}{V_t(t)}$
$f_t(t) = \lim_{h\to 0} \frac{1}{h} ln(E[e^{\int_t^{t+h} (\mu_u - r - \frac{1}{2}\sigma_u^2) 1_{\{\tau^* \geq u\}} du + \int_t^{t+h} \sigma_u 1_{\{\tau^* \geq u\}} dW_u} | F_t])$
$f_t(t) = \lim_{h\to 0} \frac{1}{h} ln E(1 + \int_t^{t+h} (\mu_u - r - \frac{1}{2}\sigma_u^2) 1_{\{\tau^* \geq u\}} du + \int_t^{t+h} \sigma_u 1_{\{\tau^* \geq u\}} dW_u)$
$f_t(t) = \mu_u - r - \frac{1}{2}\sigma_u^2$. □

2.3.3 Stopping time

In this subsection, we will discuss the new stopping time associated with multiplicative model.

Assume V_t is given by (2.35). Let the forward drift process $f(t,T)$ be given by (2.28) under the conditions (2.29) and (2.30). Let the dynamics of G_t be given by (2.33) under the conditions (2.24) and(2.25). Note that $V_t \geq G_t$ in continuation region. Therefore, $e^{\int_t^T f_t(u)du} \geq 1$. Hence,
$\int_t^T f_t(u)du \geq 0$. Therefore, it is optimal time to stop the value process is when $\int_t^T f_t(u)du \leq 0$. In other words,the optimal stopping time of the value process is

$$\tau^* = \inf\{t \leq s \leq \tau : \int_s^T f_s(u)du \leq 0\} \tag{2.36}$$

2.3.4 No arbitrage drift condition

Now let's take a look at the no arbitrage drift restriction for the multiplicative model.

Theorem 4. *Assume V_t defined by* (2.35)*, the forward drift process $f(t,T)$ is given by* (2.28) *under the conditions* (2.29) *and* (2.30)*. Let the dynamics of G_t be given by* (2.33) *under the conditions* (2.24) *and* (2.25)*. Then no arbitrage drift condition for the multiplicative model is $\alpha_t(T) = -\beta_t(T)(\int_t^T \beta_t(u)du + \sigma_t)$ a.e on $[0,\tau^*]$.*

Proof. Let's consider the discounted value process $\{e^{-rt}V_t\}$, where $t \geq 0$. Therefore, $e^{-rt}V_t = G_t e^{\int_t^T f_t(u)du - rt}$. Let $A(t) = e^{\int_t^T f_t(u)du - rt}$.
so we have,

$$
\begin{aligned}
d(e^{-rt}V_t) &= d(G_t e^{A(t)}) \\
&= G_t d(e^{A(t)}) + e^{A(t)} dG_t + dG_t de^{A(t)} \\
&= e^{A(t)} G_t ((\int_t^T \alpha_t(u)du - f(t,t) - r)dt + (\int_t^T \beta_t(u)du)dW_t + \frac{1}{2}(\int_t^T \beta_t(u)du)^2 dt + \mu_t dt + \\
&\quad \sigma_t dW_t + \sigma_t (\int_t^T \beta_t(u)du)dt) \\
&= e^{A(t)} G_t ((\int_t^T \alpha_t(u)du - f_t(t) - r + \mu_t + \sigma_t \int_t^T \beta_t(u)du + \frac{1}{2}(\int_t^T \beta_t(u)du)^2)dt + \\
&\quad (\int_t^T \beta_t(u)du + \sigma_t)dW_t)
\end{aligned}
$$

Since $e^{-rt}V_t$ is a martingale on continuation region,

$\int_t^T \alpha_t(u)du = f_t(t) - \mu_t - r - (\sigma_t \int_t^T \beta_t(u)du + \frac{1}{2}(\int_t^T \beta_t(u))^2)$. But $f_t(t) = \mu_t - r - \frac{1}{2}\sigma_u^2$ by theorem 3. Therefore,

$\int_t^T \alpha_t(u)du = -(\sigma_t \int_t^T \beta_t(u)du + \frac{1}{2}(\int_t^T \beta_t(u))^2 + \frac{1}{2}\sigma_u^2)$.

By taking the differential with respect to T

$\alpha_t(T) = -\beta_t(T)(\int_t^T \beta_t(u)du + \sigma_t)$ a.e on $[0, \tau^*]$. This completes the proof. □

2.4 Calibration

Main advantage of forward modeling approach is calibration. HJM method facilitate calibration via taking the initial forward curve as an input to the model dynamics. We will address how calibration is done for additive and multiplicative models in detail under chapter 3.

In the following section, we will discuss a detailed example of additive model applied to put option. Here we will present the solution to the optimal stopping problem of American put option, stopping criteria and the stopping time using forward modeling approach.

2.5 Put option price using additive model

Let's consider the discounted value process of finite horizon optimal stopping problem. Solution can be found by solving

$$V_t = \operatorname*{ess\,sup}_{t\leq\tau\leq T} E[e^{-r(\tau-t)}G_\tau|F_t]$$
$$\tau^* = \inf\{t \leq s \leq T : V_s = G_s\}$$

where $E(\sup_{0\leq t\leq T}|G_t|) < \infty$ and τ^* is the optimal stopping time.
According to our model, the value function V_t is given by (2.35), the dynamics of forward drift $f_t(u)$ is given by (2.28), the dynamics of G_t is given by (2.33) and the optimal stopping time τ^* is given by equation (2.36). consider,

$e^{-rt}V_t = \operatorname*{ess\,sup}_{t\leq\tau\leq T} E[e^{-r\tau}G_\tau|F_t]$

Since,

$$\begin{aligned} e^{-r\tau^*}G_{\tau^*} - e^{-rt}G_t &= \int_t^\tau d(e^{-ru}G_u) \\ &= \int_t^{\tau^*} (-re^{-ru}G_u du + e^{-ru}dG_u) \\ &= \int_t^{\tau^*} e^{-ru}(-rG_u + \mu_u du + \sigma_u dW_u) \\ &= \int_t^{\tau^*} e^{-ru}((\mu_u - rG_u)du + \sigma_u dW_u) \end{aligned}$$

Now consider for $t \leq \tau^* \leq T$,

$$
\begin{aligned}
E[e^{-r(\tau^*-t)}G_{\tau^*}|F_t] &= e^{rt}E[e^{-r\tau^*}G_{\tau^*}|F_t] \\
&= e^{rt}(e^{-rt}G_t + E[\int_t^{\tau^*} e^{-ru}(\mu_u - rG_u)du|F_t] + E[\int_t^{\tau^*} e^{-ru}G_u dW_u|F_t]) \\
&= G_t + e^{rt}E[\int_t^{\tau^*} e^{-ru}(\mu_u - rG_u)|F_t] \\
&= G_t + E[\int_t^{T} e^{-r(u-t)}(\mu_u - rG_u)1_{\{\tau^*\geq t\}}|F_t]
\end{aligned}
$$

So the forward drift is given by

$f_t(u) = E[\int_t^T e^{-r(u-t)}(\mu_u - rG_u)1_{\{\tau^*\geq t\}}|F_t]$.

Let $G_t = (K - S_t)^+$ and let $dS_t = S_t(rdt + bdW_t)$ where r is the risk free interest rate and b is the volatility.

By Meyer-Tanaka formula we have,

$(K - S_u)^+ = (K - S_0)^+ - \int_0^u 1_{\{S_x<K\}}dS_x + \frac{1}{2}L_u^K(S_x)$, where $t \leq x \leq u$.

Since American put has an early exercise boundary l where $l \leq K$, local time spent at level K, $L_u^K(S_x)$ is zero on the event $\{\tau^* \geq u\}$.

Therefore,

$$
\begin{aligned}
d(K - S_t)^+ &= -d\int_0^u 1_{\{K>S_x\}}dS_x \\
&= -1_{\{l>S_u\}}(rS_u du + bdW_t) \\
&= -rS_u 1_{\{l>S_u\}}du - bS_u 1_{\{l>S_u\}}dW_u
\end{aligned}
$$

We will use the differential $d(K-S_t)^+$ to calculate $f_t(u)$ given in following theorem.

Theorem 5. *Let dynamics of $f_t(u)$ be given by* (2.28) *under the conditions* (2.29) *and* (2.30). *Let dynamics of G_t be given by* (2.23) *under the conditions* (2.24) *and* (2.25). *Then the forward drift for American put with payoff $(K - S_t)^+$ is given by*

equation (2.41) *and the optimal stopping time is given by equation* (2.42)

Proof. Since $V_t = G_t + \int_t^T E[e^{-r(u-t)}(\mu_u - rG_u)1_{\{\tau^* \geq t\}}du|F_t]$ forward drift $f_t(u)$ is given by

$f_t(u) = E[e^{-r(u-t)}(\mu_u - rG_u)1_{\{\tau^* \geq t\}}du|F_t]$

Since $G_t = (K - S_t)^+$

$f_t(u) = E[e^{-r(u-t)}(-rS_u 1_{\{l > S_u\}}du - r(K - S_u)^+)1_{\{\tau^* \geq u\}}|F_t]$.

Let $A = E[e^{-r(u-t)}(K - S_u)^+ 1_{\{\tau^* > u\}}|F_t]$ and $B = E[e^{-r(u-t)}S_u 1_{\{l > S_u\}}1_{\{\tau^* > u\}}|F_t]$ for the sake of simplicity. So $f_t(u) = -rA - rB$. Let's try to calculate A and B separately. Note that

$dS_u = S_u(rdt + bdW_t) \implies G_t = S_u e^{(r - \frac{1}{2}b^2)(u-t) + bW_{u-t}}$.

Let $\underset{t \leq m \leq u}{\text{Max}} = M_u$. Then $\{\tau > u\} \Leftrightarrow \{M_u < l\}$.

This follows,

$1_{\{\tau > u\}} \Leftrightarrow 1_{\{l > M_u\}}$.

Consider, $S_u = S_t e^{b\hat{W}_{u-t}}$ where $\hat{W} = \rho t + W_t$, $\rho = \frac{r}{b} - \frac{b}{2}$.

Let $M_u = \underset{t \leq m \leq u}{\text{Max}} S_t e^{b\hat{W}_{u-t}} = S_t e^{b\hat{W}_{u-t}}$. Also $\hat{M}_u = \underset{t \leq m \leq u}{\text{Max}} \hat{W}_m$.

Lets calculate A first. Recall,

$$\begin{aligned} A &= E[e^{-r(u-t)}(K - S_u)^+ 1_{\{\tau^* > u\}}|F_t] \\ &= E[e^{-r(u-t)}(K - S_u)^+ 1_{\{M_u < l\}}|F_t] \end{aligned}$$

Notice that A is a barrier put option. Let's calculate it using barrier call option price and put - call parity. Let $C(t, S_t, l)$ be the barrier call price.Then

$$C(t, S_t, l) = E[e^{-r(u-t)}(S_u - K)^+ 1_{\{M_u < l\}} | F_t] \tag{2.37}$$

Also consider the following

$\{M_u < l\} \Leftrightarrow \{\hat{M}_u < l^*\}$, where $l^* = \frac{1}{b} ln(\frac{l}{S_t})$.

$\{S_u > K\} \Leftrightarrow \{\hat{W}_u > K_*\}$, where $K^* = \frac{1}{b} ln(\frac{K}{S_t})$. According to Shreve (2000), the joint density function under risk neutral measure for $(\hat{M}_u, \hat{W}_u)$ is given by

$$f_{(\hat{M}_u, \hat{W}_u)}(m, w) = \frac{1}{T\sqrt{2\pi T}} = e^{\rho w - \frac{1}{2}\rho^2 T - \frac{1}{2T}(2m-w)^2} \tag{2.38}$$

where $w \leq m$, $m \geq 0$ and $T = u - t$.

Let's recall the barrier call price (2.37),

$$\begin{aligned} C(t, S_t, l) &= E[e^{-r(u-t)}(S_u - K)^+ 1_{\{M_u < l\}} | F_t] \\ &= E[e^{-r(u-t)}(S_u - K) 1_{\{\hat{M}_u < l^*, \hat{W} > K_*\}} | F_t] \end{aligned}$$

Shreve (2000), formulation of barrier call option price and it's solution are given by

$$C(t, S_t, l) = \int_{K^*}^{l^*} \int_{w \vee 0}^{l^*} e^{-rT}(K - S_t e^{bw}) \frac{2(2m-w)}{T\sqrt{2\pi T}} e^{\rho w - \frac{1}{2}\rho^2 T - \frac{1}{2T}(2m-w)^2} dm dw \tag{2.39}$$

Where $T = u - t$.

$$C(t, S_t, l) = S_t I_1 - K I_2 + S_t I_3 - K I_4 \tag{2.40}$$

$$\begin{aligned} I_1 &= N(\delta_+(T, \frac{S_t}{K})) - N(\delta_+(T, \frac{S_t}{l})) \\ I_2 &= e^{-rT}(N(\delta_-(T, \frac{S_t}{K})) - N(\delta_-(T, \frac{S_t}{l}))) \\ I_3 &= (\frac{S_t}{l})^{\frac{2r}{b^2}-1}(N(\delta_+(T, \frac{l^2}{KS_t})) - N(\delta_+(T, \frac{l}{S_t}))) \\ I_4 &= e^{-rT}(\frac{S_t}{l})^{\frac{2r}{b^2}+1}(N(\delta_-(T, \frac{l^2}{KS_t})) - N(\delta_-(T, \frac{l}{S_t}))) \end{aligned}$$

Using put - call parity,

$$e^{-rT}(S_u - K)^+ - e^{-rT}(K - S_u)^+ = e^{-rT}(S_u - K)$$

$$e^{-rT}(S_u - K)^+ 1_{\{\tau^* > u\}} - e^{-rT}(K - S_u)^+ 1_{\{\tau^* > u\}} = e^{-rT}(S_u - K)1_{\{\tau^* > u\}}$$

$$E[e^{-rT}(S_u - K)^+ 1_{\{\tau^* > u\}}|F_t] - E[e^{-rT}(K - S_u)^+ 1_{\{\tau^* > u\}}|F_t] = E[e^{-rT}(S_u - K)1_{\{\tau^* > u\}}|F_t]$$

Therefore, $C(t, S_t, l) - E[e^{-rT}(S_u - K)1_{\{\tau^* > u\}}|F_t] = A$. Plugging A and B into forward drift $f_t(u) = -rA - rB$ we have,

$$\begin{aligned} f_t(u) &= -rC(t, S_t, l) + rE[e^{-rT}(S_u - K)1_{\{\tau^* > u\}}|F_t] - rE[e^{-r(u-t)}S_u 1_{\{l > S_u\}} 1_{\{\tau^* > u\}}|F_t] \\ &= -rC(t, S_t, l) + rE[e^{-rT}(S_u - K)1_{\{\tau^* > u\}}|F_t] - rE[e^{-rT}S_u 1_{\{\hat{M} < l^*\}}|F_t] \\ &= -rC(t, S_t, l) - rKE[e^{-rT}1_{\{\hat{M} < l^*\}}|F_t] \\ &= -rC(t, S_t, l) - rKP\{\hat{M} < l^*\} \end{aligned}$$

By corollary 7.2.2 Shreve (2000),
$P\{\hat{M} < l^*\} = N(\frac{l^* - \rho t}{\sqrt{T}}) - e^{2\rho l^*} N(\frac{-l^* - \rho t}{\sqrt{T}})$, where $l^* \geq 0$.
Therefore we have forward drift process calculated as

$$f_t(u) = -rC(t, S_t, l) - rKN(\frac{l^* - \rho t}{\sqrt{T}}) - e^{2\rho l^*} N(\frac{-l^* - \rho t}{\sqrt{T}}) \tag{2.41}$$

where $C(t, S_t, l)$ is the barrier call option price. Therefore, we can express American put value process in terms of forward drift explicitly as
$V_t = G_t + \int_t^T f_t(u)du$ where $G_t = (K - S_t)^+$. Finally,
$V_t = (K - S_t)^+ + \int_t^T f_t(u)du$ with $f_t(u)$ is given by the equation (2.41).
Let's take a look at the the new stopping time associated with additive model. Let's recall the optimal stopping time of the additive model is given by theorem 3. Optimal stopping time for the put option example is given by substituting $f_t(u)$ to equation

(2.36).

$$\tau^* = \inf\{t \leq s \leq \tau : \int_s^T -rC(s, S_t, l) - rKN(\tfrac{l^* - \rho s}{\sqrt{T}}) - e^{2\rho l^*} N(\tfrac{-l^* - \rho s}{\sqrt{T}})du \leq 0\} \quad (2.42)$$

□

This completes the example for American put option under additive model.

CHAPTER 3: IMPLEMENTATION OF ADDITIVE MODEL

In this chapter, we will implement additive model for the American put option on IBM stock index. We analyze the market data under three main techniques. Carmona, Ma, Nadtochiy (2015) implemented the forward modeling approach for implied volatility surface. We follow their forward model dynamics for forward drift modeling. As Carmona, Ma, Nadtochiy (2015) we will use principal component analysis as one of the techniques for our analysis. Further we analyze data using robust principal component analysis and Karhunen - Loeve decomposition. First, we will introduce solution method to the additive model.

3.1 Solution method

Recall the forward drift for the additive model is given by

$$f_t(u) = \frac{\partial(V_t - G_t)}{\partial T}$$

as in equation (2.27).

Therefore we have

$$df_t(u) = \frac{\partial}{\partial t}(\frac{\partial(V_t - G_t)}{\partial T}) \tag{3.43}$$

Also note that the dynamics of $f_t(u)$ is given by $df_t(u) = \alpha_t(u)dt + \beta_t(u)dW_t$ as in equation (2.28) under the conditions (2.29) and (2.30). As in Carmona, Ma, Nadotchiy (2015), we will try to model $f_t(u)$ directly as

$$f_t(u) = f_0(T) + \int_0^t \alpha_u(T)du + \sum_{n=1}^{m} \int_0^t \beta_u^n(T)dW_u^n \tag{3.44}$$

Where n is the number of Brownian factors. Also $\alpha_u(t)$ and $\beta_u^n(t)$ satisfy conditions (2.29) and (2.30).

3.1.1 Dynamics of additive model

Note that in additive model $\int_0^t \alpha_t(u)du = 0$. Therefore, dynamics of the forward drift that we seek to model is given by

$$f_t(u) = f_0(T) + \sum_{n=1}^{m} \int_0^t \beta_u^n(T)dW_u^n \tag{3.45}$$

We seek to model the volatility $\beta_t^n(u)$ by applying principal component analysis for $df_t(u)$ of the additive model. Which is given in equation (3.43)

$$df_t(u) = \frac{\partial}{\partial t}(\frac{\partial(V_t - G_t)}{\partial T})$$

3.1.2 Market data and data preparation

Our model requires both American type option prices V_t and corresponding index payoff G_t. Market data of the American put option prices on IBM index prices is obtained through Option Matrix database. Stock prices of IBM index is obtained through Crisp database. Access to these databases is provided through WRDS database. Our data streams consider options and index data from 08/01/2007 to 08/31/2015. First step of the data preparation process is the calculation the payoff of the IBM index value G_t, since it is not readily available to us. Then we matched V_t and G_t according to the date for available data from 08/01/2007 to 08/31/2015. Our next step was to calculate forward drift $f_t(u)$ according to equation (3.43).

There were significant amount of missing data in our data set. We will use python software package to impute missing data using it's interpolate function. We carry out

our analysis on different buckets of moneyness. Moneyness of the option is defined as $m = \frac{K}{S_t}$ where K is the strike price and S_t is the IBM index price. Then We will carry out our analysis when option is in the money, on the money and out of the money categories.

3.1.3 Model implementation

Let observation dates of $f_t(u)$ denoted by t_j and $t_j < t_{j+1}$ where $j = 1, 2, 3...J$. Let forward rates were observed for relative maturities $\tau_m = T_m - t_j$ where T_m is the maturities with $m = 1, 2, 3..M$.

Now we introduce $f_{t_j}(\tau_m)$ as the forward rate observed at t_j for relative maturity τ_k. We calculate the difference matrix of forward drift In the next step as in equation (3.31). Here $\delta > 0$ such that $t_j + \delta < t_{j+1}$.

$$\Delta f_t(\tau_m) = f_{t_j+\delta}(\tau_m) - f_{t_j}(\tau_m) = y_{j,m} \tag{3.46}$$

For J number of observations over K different relative maturities, we can represent the data matrix Y calculated according to (3.46).

$$Y = \begin{bmatrix} y_{1,1} & y_{2,1} & & & y_{j,1} \\ y_{2,1} & \ddots & \ddots & \ddots & \\ y_{j,1} & \ddots & \ddots & \ddots & \ddots \\ & \ddots & \ddots & \ddots & \ddots \\ y_{J,1} & & \ddots & \ddots & _{J,M} \end{bmatrix}, \text{ where } Y \in \mathcal{R}^{J \times M}.$$

We set δ to be one trading day. Observation dates t_j to be the first day of each week of trading. Same as Carmona, Ma, Nadtochiy(2015), our goal is to choose the volatility terms β_t^n to match the covariance matrix of Y. This is achieved by applying

principal component analysis to the covariance matrix of Y.

3.1.4 Principal component decomposition and data analysis

principal component decomposition of covariance matrix of Y is the decomposition

$$cov(Y) = CDC^{\mathsf{T}} \tag{3.47}$$

Where C is $M \times M$ eigen vector and D is the diagonal matrix of size $M \times M$ which comprise of eigen values of the decomposition. Principal component decomposition is a statistical technique that attempt to uncover the variance in high dimensional data. This procedure is designed to project multidimensional data into orthogonal axis's which are linear combinations of original dimensions of the given data set. Eigen value gives the variation of original data along these new axis's. This procedure is useful for extracting information such as variance from high dimensional data. Another advantage of Principal component analysis is that it reduces the dimension of high dimensional data. In depth discussion of the principal component decomposition can be found in Abidi, Williams (2010). Applying principal component analysis to the covariance matrix of the difference matrix Y, we found that first three eigen modes explain over 92% of the variance.

Table 3.1: Variance explained by eigen modes

Eigen mode	Variance
1	53.44%
2	20.65%
3	18.54%

Therefore, we use only three Brownian factors in further analysis. Researchers and practitioners have noticed that first three eigen components describe special characteristics of the yield curve. These shapes have an interpretative meaning. They tell us how the yield curve react to different market shocks in interest rate modeling.

Historical researches suggest that the first component typically represents a parallel shift in the yield curve. Second and third components represent a twist and a bend in the yield curve. As an example, Svensson (1994) noticed that first eigen mode shows a parallel shift in yield curve and second eigen component shows an inverted or twisted shape.

Similar effects can be observed for eigen mode analysis of the implied volatility surface. Historical observations suggest that first eigen component represents a parallel shift, second eigen component represents a twist in the volatility curve. Skiadopoulos,Hodges, Clewlow (1999) have observed similar results for the first two eigen modes in their analysis of S&P 500 implied volatility surface of American options. Cont and Fonseca (2006) have observed similar behavior for first two eigen modes same as Skiadopoulos, Hodges, Clewlow (1999). They used Karhunen - Loeve transformation to investigate the behavior of implied volatility surface. They further observed that the third eigen mode shows butterfly effect. Butterfly effect is a result of change in convexity of the implied volatility surface . Cont and Fonseca (2006).

We will analyze the shapes of the first three eigen components for the forward drift process in this section. Our goal is to investigate the shapes of first three eigenmodes and their inferences for additive model. Skiadopoulos, Hodges and Clewlow (1999) and Cont and Fonseca (2006) noticed that there is a variation of shapes of the eigen components according to the moneyness. Therefore we consider three maturity buckets in this analysis. Let $.8 \leq m \leq 1.2$ be the on the money bucket. Let $.4 \leq m < .8$ be the out of the money bucket and let $1.2 < m \leq 1.5$ be the on the money bucket.

3.1.5 Eigen component analysis for out of the money bucket

First three eigenmodes given by the principal decomposition of the covariance matrix for out of the money bucket is depicted in the following graph. Solid line represents the second eigen component. Solid line with circles is the first eigen component and

the solid line with squares is for the third eigen component.

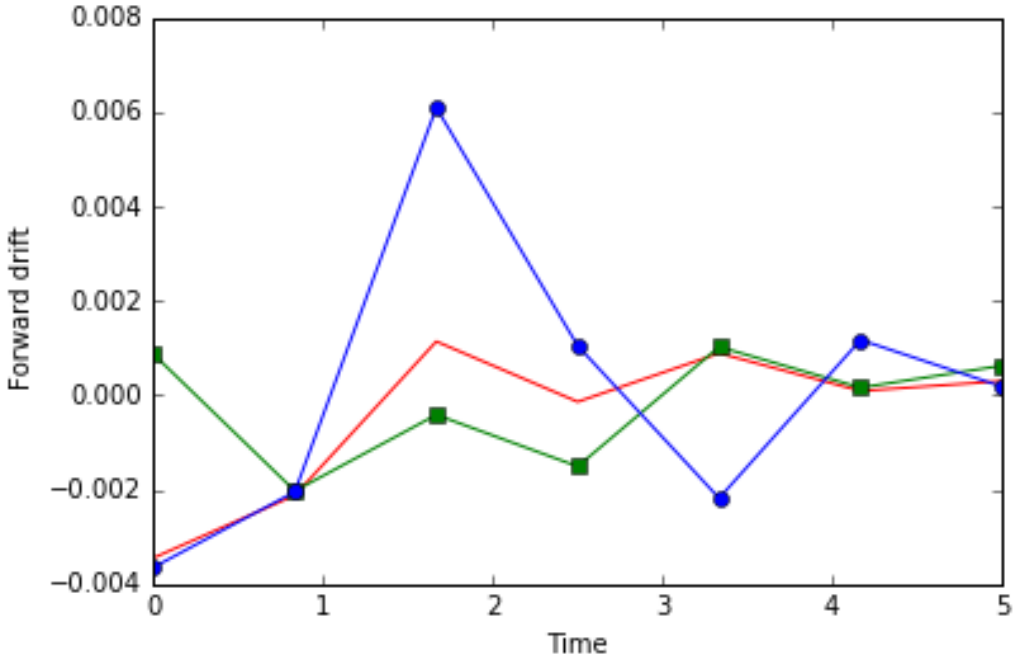

Figure 3.2: Eigen component for out of the money bucket

We can see that the first eigen component is given by the solid line with circles show neither a constant nor a butterfly shape. It does tend to move in opposite direction of other two eigen components. But the second eigen component given by the solid line tends to shows a higher variation for shorter maturities but it tends to vary less for larger maturities. It looks like that the second eigen component is converging to a constant value. Our calculations show that value to be 0.00079. This suggests that parallel shift in drift curve of 0.00079. This observation of parallel shift of the second eigen component is consistent with known historical observations for yield curve and implied volatility surface. Third eigen component is given by the solid line with squares. This line shows a butterfly shape just as in the third eigen component of implied volatility surface observed by Cont, Fonseca (2006).

3.1.6 Eigen component analysis for on the money bucket

Following graph shows the behavior of first three eigen components of the covariance matrix of Y for on the money bucket.

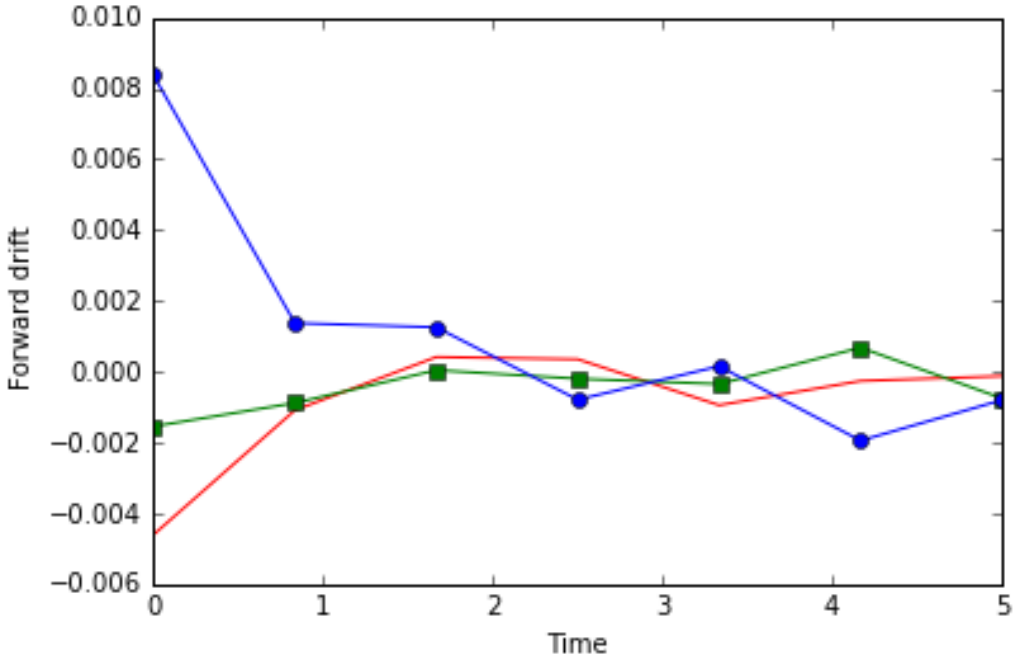

Figure 3.3: Eigen component for on the money bucket

It can be seen that first eigen component given by the line with circles, tend to move in opposite direction of other two eigen components. Implication is that the first component is highly uncorrelated to the other two components. Second eigen component is given by the solid line is close to being constant. Butterfly effect in the third eigenmode is not apparent for on the money bucket.

3.1.7 Eigen component analysis for in the money bucket

We dedicate this subsection to the analysis of in the money bucket. Graphical representation of eigen component is given in the following graph.

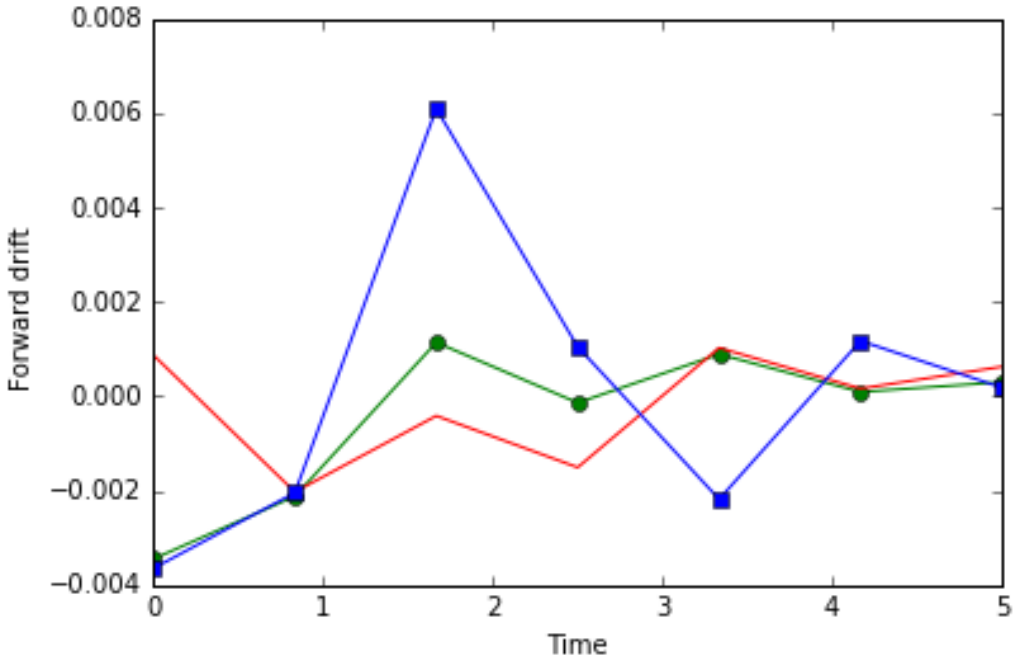

Figure 3.4: Eigen modes for in the money bucket

Just as in out of the money bucket, second eigen component given by the solid line tends to be a constant over time. This is not apparent for shorter maturities but the curve tends to vary less for larger maturities. Similarly, the third eigen component given by the solid line with squares tends to show a butterfly effect. First eigen component tend to move in opposite direction of the first two components for $T > 2.5$ years.

3.1.8 Overview of eigen component behavior for additive model for PCA

We have shown the behavior of the eigen components according to each maturity bucket. Our analysis carried out using principal component analysis. Previous research from Skiadopoulos, Hodges and Clewlow (1999) suggests that the first eigen component shows a parallel shift in yield curve analysis. Cont and Fonseca (2006) also observed similar behavior for the first eigen component for implied volatility

surface. We have observed the second eigen component, not the first one shows a parallel shift for forward drift curve. This is consistent over all moneyness buckets. The third eigen component of the forward drift curve takes a butterfly effect for all three buckets considered in our analysis. This observation is consistent with what Cont and Fonseca (2006) and Skiadopoulos,Hodges and Clewlow (1999). Main difference between our results and the historical observations lie in the behavior of the first eigen mode. First eigen component in our model move in the opposite direction of other two eigen modes, especially for larger maturities.
Another observation is that second and third eigen modes move similar to each other. This implies a higher degree of correlation among them.

Also Cont and Fonseca (2006) also noticed a mean reverting behavior of eigen modes of volatility surface. Similar behavior is apparent for eigen modes of forward drift process under all three maturity buckets.

3.2 Eigen mode analysis using robust principal component analysis

Robust principal component analysis is similar to principal component analysis but it can be applied to corrupt or missing data. It does take the data matrix as it is with or without missing data while preserving the original dimensions. Note that regular principal component analysis requires the data matrix to be complete. Procedure does not allow to have missing values in the data matrix. There are several ways to deal with the missing data. One method is imputation through regression function or interpolation. Another method is to replace the missing data with the mean value of the available data or simply discard the missing values. Missing data needs to be dealt with careful attention because it can leads to misleading conclusions. Since our data consists of over 10% percent of missing data, it is very important that we do not overlook the effect of missing data. Note that even though we impute the missing data, it is better to analyze the effect of missing data if there is any. Further

discussion about robust principal component analysis can be found in Candes, Li, Ma and Wright(2009).

3.2.1 Robust principal component analysis for out of the money bucket

We use robust principal component analysis for out of the money maturity bucket. Eigen components plot is given by the following graph.

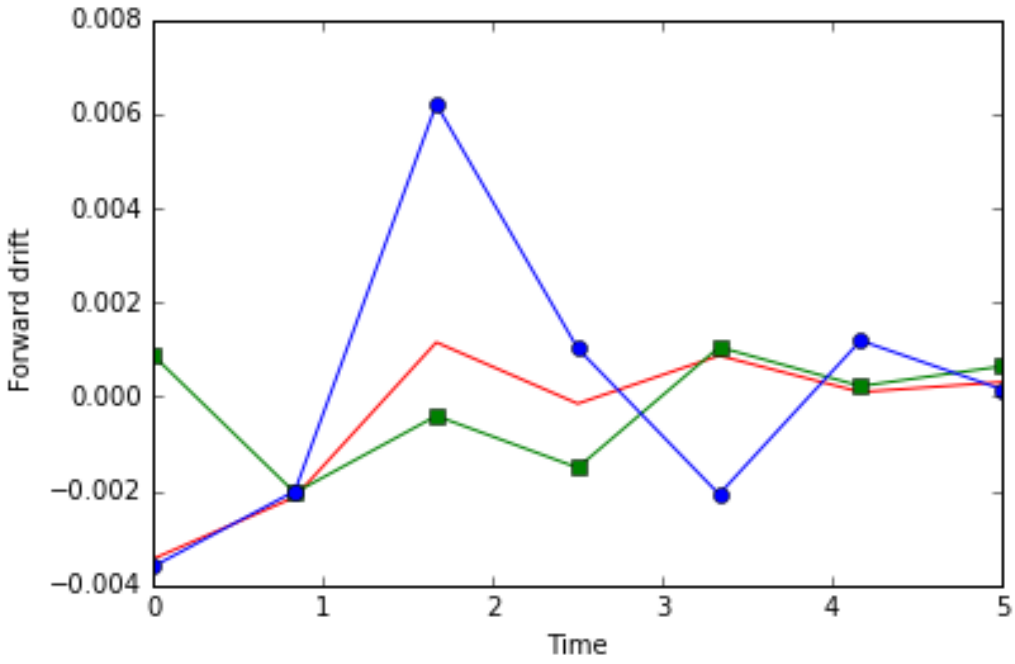

Figure 3.5: Eigen modes for out of the money bucket using robust PCA

First eigen component given by the solid line with circles tends to move against the other two for larges maturities. Second eigen component given by solid line tends to converge to a constant as we observed in regular principal component analysis. Moreover, third eigen component shows a butterfly effect as we would expect. Curves for eigen components under the robust principal component analysis is very similar to the curves under regular principal component analysis. This suggest that the effect of missing data and imputation has minimal effect.

3.2.2 Robust principal component analysis for on the money bucket

Plots of first three eigen components under on the money bucket is given in the following graph.

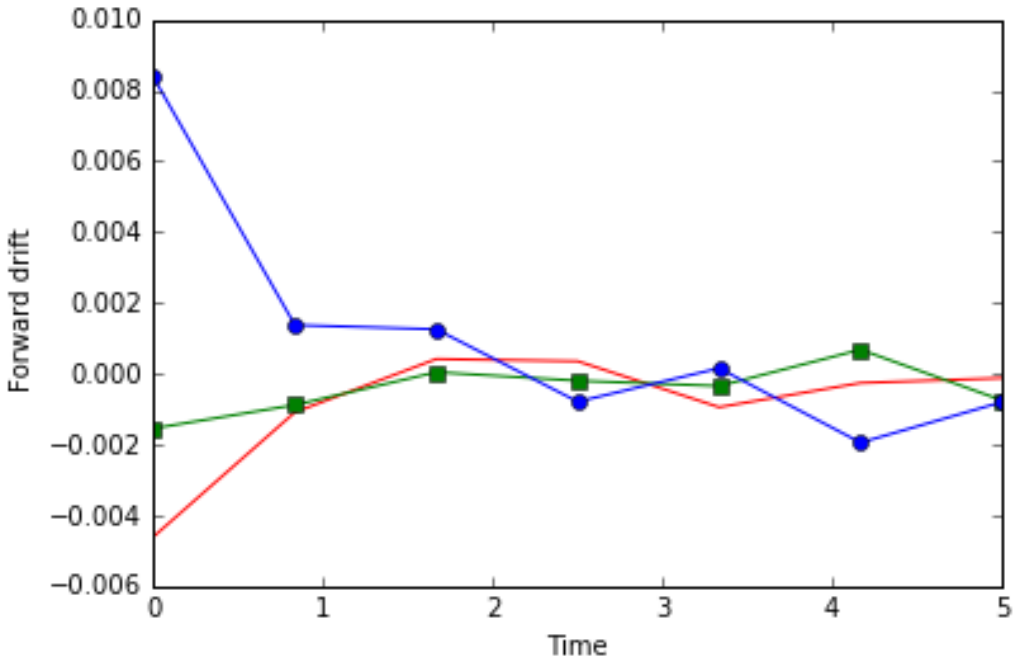

Figure 3.6: Eigen modes for on the money bucket using robust PCA

Similar behavior of eigen components to regular principal component analysis can be seen here. Graphs are almost identical as well. Second eigen component curve which is given by the solid line tends to look like a constant. Butterfly effect is not clearly visible here as we saw in regular principal component case. Movement of the first component is clearly in the opposite directions of the other two suggesting that they are highly uncorrelated.

3.2.3 Robust principal component analysis for in the money bucket

Eigen modes plots for in the money bucket is given in the following graph. Robust principal component yields an almost identical graph for same moneyness bucket

under regular principal component analysis. We already observed this pattern over other two moneyness buckets as well.

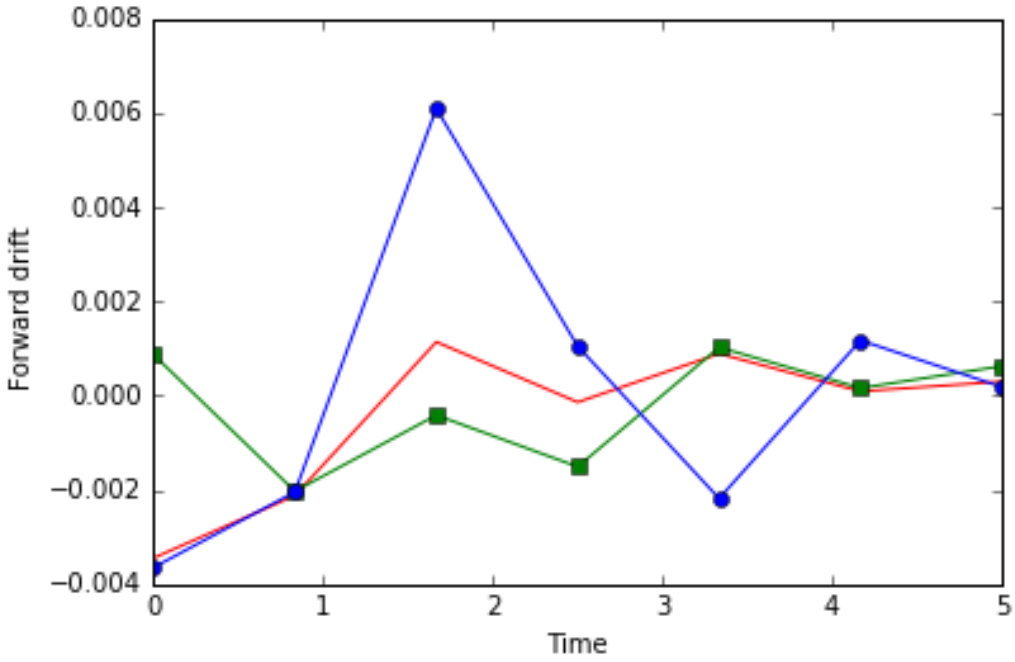

Figure 3.7: Eigen modes for in the money bucket using robust PCA

Note that the second eigen component given by the solid line tends to be a constant over time. Butterfly effect of the third component which is given by the solid line with squares is also clearly visible. First eigen component show a movement against the other two components especially for larger maturities.

3.2.4 Overview of robust principal component analysis

Missing data in the original data set led us to use robust principal component analysis. We used interpolate function in python numpy package to impute missing data. Regular principal component decomposition results we obtained was very closely matched by the robust principal component analysis. This suggests that effect of missing data is very minimal for the data set we considered.

3.3 Karhunen-Loeve (KL)transformation

KL tranaformation is a data analysis technique widely used in signal processing and machine learning. It is similar to principal component analysis but it tends to explain variation within data for higher dimensional random fields. Considering the fact that the data matrix of daily volatility differences as a random field, Cont and Fonseca (2006) applied Karhunen-Loeve transformation to the implied volatility surface given by SP index and FTSE data. Since our data matrix of forward differences can be thought of as a random field, we employ Karhunen-Loeve transformation for our analysis. More details about the eigen surface, KL transform and it's implementation can be found in sections 3.3 and 3.4 of Cont and Fonseca (2006). We apply our data to eigen surface given by equation 21 in their paper. They further used Nadaraya-Watson estimator given in equation 7 and Gaussian kernel to obtain a smooth eigen surface. We also use the implementation of KL transformation of random fields by Dubourg (2013) to aid our analysis. This results in the following eigen surface.

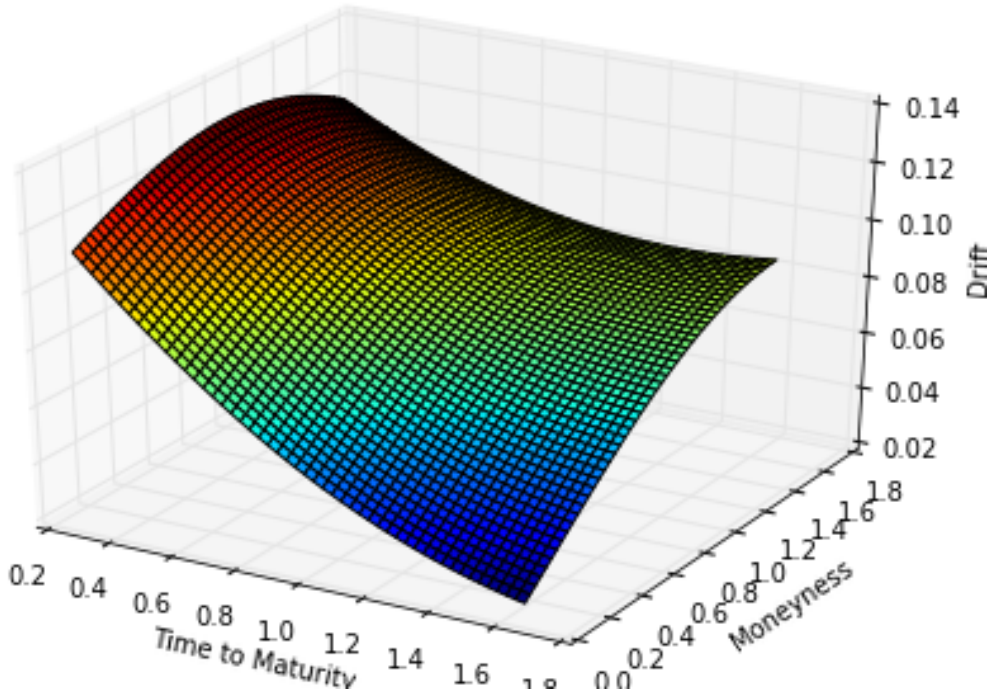

Figure 3.8: Eigen surface for forward drift process under additive model

3.4 Forward drift simulation for additive model

We will simulate the forward drift for the additive model in this section. Initial forward vector $f_0(T)$ is given by the following vector observed by market data. Data available for 13 maturities. Initial vector is given by

$f_0(T) = [0.020058, 0.010608, 0.001523, 0.000265, 0.001108, -0.010265, 0.000115, -0.000221, 0.001095, -0.0002112, 0.000431, -0.000220, 0.000332]$

Here we consider the simulation for $T = 1$ year or 252 trading days for our demonstration. Let's recall the forward drift curve is given by (3.28) as

$$f_t(u) = f_0(T) + \sum_{n=1}^{m} \int_0^t \beta_u^n(T) dW_u^n$$

We established that over 92% of the variation in the data set is captured by the first three eigen components. Therefore, we will use three Brownian factors in our analysis. These factors $\beta_u^n(T)$ are estimated by the corresponding eigen components as deterministic functions.

3.4.1 Estimation of volatility functions

Second eigen component of principal component decomposition consistently showed a constant shape with time across the three maturity buckets. Therefore, we can estimate the second eigen mode by a constant function by taking the average across three buckets. Estimation of exact functional form of first and the third eigen component is difficult since they do not appear to take a simple functional form. However they both tend to show a mean reverting behavior. This is consistent for all three maturities we considered. Therefore, we may estimate them by their mean value. Estimated volatility functions are given in the following table.

Table 3.2: Estimation of volatility functions for additive model

Eigen mode	Variance
$\beta_u^1(T)$	-0.00043
$\beta_u^2(T)$	0.00081
$\beta_u^3(T)$	0.000232

Simulation of the forward drift curve was carried out using above volatility functions, initial forward drift $f_0(T)$ and the simulation equation given by (3.28). Formally,

$$f_t(u) = f_0(T) - \int_0^t 0.00043 dW_u^1 + \int_0^t 0.00081 dW_u^2 + \int_0^t 0.000232 dW_u^3 \qquad (3.48)$$

Where dW_u^1, dW_u^2, dW_u^3 are uncorrelated Brownian motions.

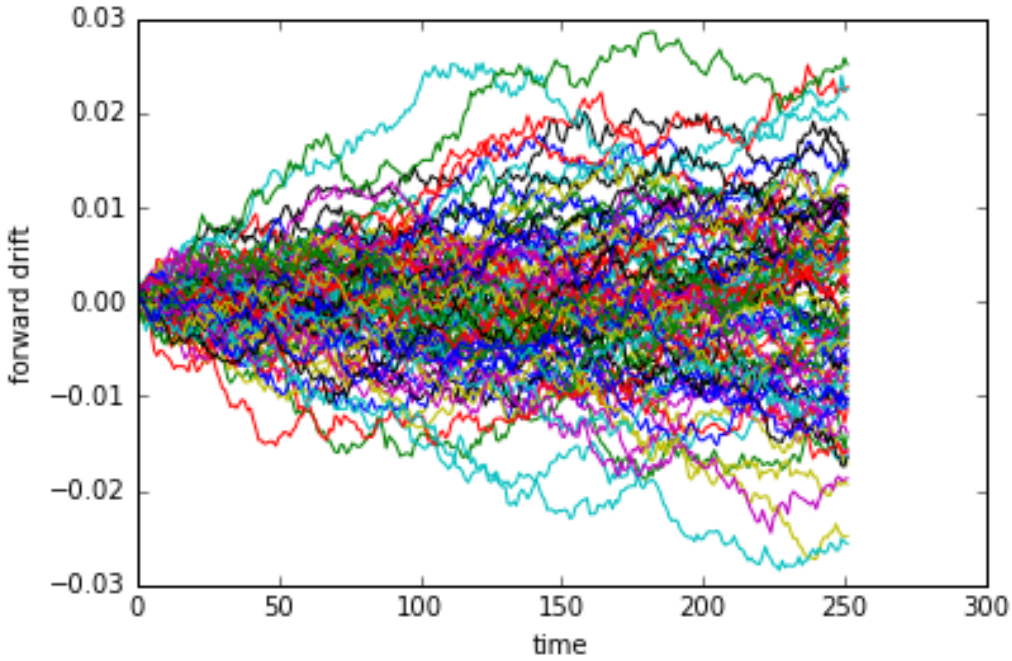

Figure 3.9: Simulation of the forward drift process

Next, we will demonstrate how to numerically estimate the optimal stopping time for the additive model for above simulation run. Let's recall the optimal stopping time τ^*, which is given by theorem 3.

$$\tau^* = \inf\{t \leq s \leq \tau : \int_s^T f_s(u)du \leq 0\}.$$

Above simulation run contain 100 paths of $f_t(u)$. $\int_s^T f_s(u)du$ was calculated for the curve given by taking the average of those 100 paths.Our calculations of integral yields the following graph.

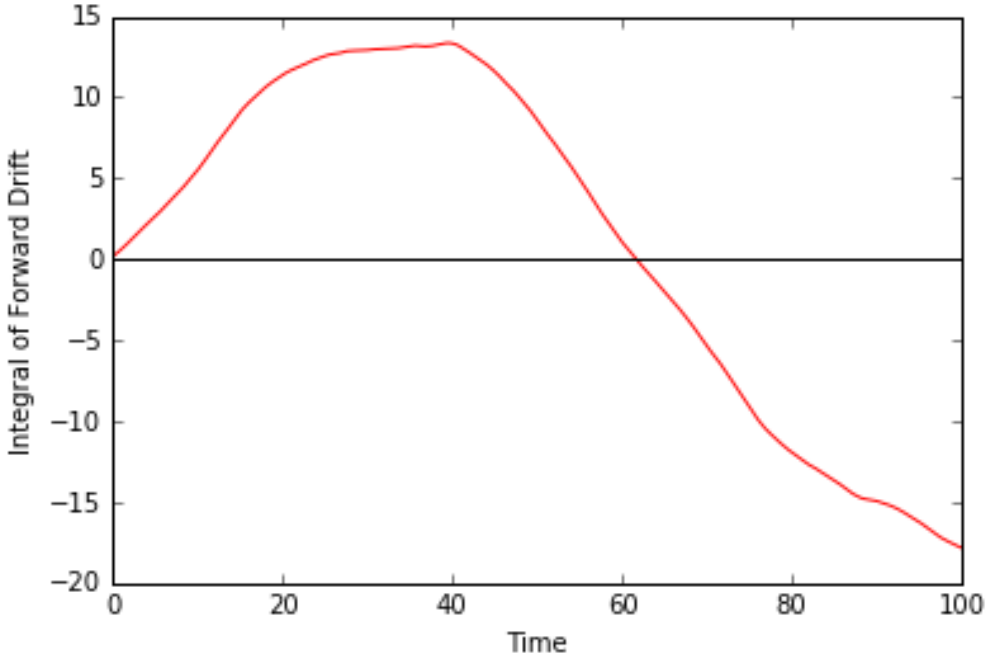

Figure 3.10: Integral of the forward drift process and stopping time

Our simulation suggests that at time index $s = 18$ is the first time $\int_s^T f_s(u)du \leq 0$. Therefore $\tau^* = 18$ for this simulated scenario.

We discussed the eigen mode analysis for data matrix under three different methods: principal component analysis, robust principal component analysis and Karhunen-Loeve transformation. We observed some distinct behavior in eigen modes for forward drift process compared to yield curve or implied volatility surface under additive model. We will investigate the multiplicative model in the next chapter.

CHAPTER 4: IMPLEMENTATION OF MULTIPLICATIVE MODEL

In this chapter, we will implement the multiplicative model for the American put option on IBM stock index. We analyze the market data under principal component analysis, robust principal component analysis and Karhunen-Loeve transformation as in additive model.

4.1 Solution method

Recall that the solution to the American option problem is given by $V_t = G_t e^{\int_t^T f_t(u)du}$. This implies that

$$f_t(u) = \frac{\partial}{\partial T}(ln\frac{V_t}{G_t}) \tag{4.49}$$

This leads to

$$df_t(u) = \frac{\partial}{\partial t}(\frac{\partial}{\partial T}(ln\frac{V_t}{G_t}))$$

Also note that the dynamics of $f_t(u)$ is given by $df_t(u) = \alpha_t(u)dt + \beta_t(u)dW_t$ as in equation (2.14).

Since we already have discussed the data preparation, general overview of principal component analysis in chapter 3, we can begin our discussion of eigen mode analysis. Let's turn our focus on variation in the data and how much of it is explained by the eigen modes. Our results suggests that over 93 percent of the variation explained by the first three eigen components. Therefore we only retain three eigen components in our analysis.

Table 4.3: Variance explained by eigen modes

Eigen mode	Variance
1	51.44%
2	28.65%
3	12.54%

Just as in the additive model, we will analyze the eigen components under three maturity buckets. Buckets considered here is the same as in the additive model.

4.1.1 Eigen component analysis for out of the money bucket

We will investigate the first three eigen modes in this subsection under out of the money bucket. Graph of those components is shown below.

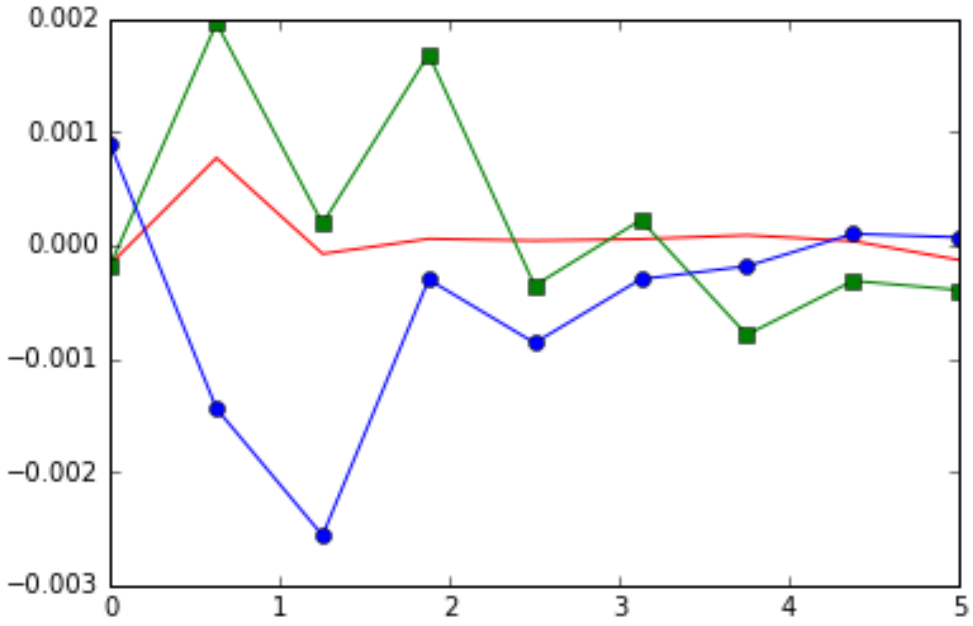

Figure 4.11: Eigen modes for out of the money bucket

Note that the first eigen component is given by the line with circles, second eigen component is given by the line with squares and the third component is given by the solid line. We can clearly see that the third eigen component tends to be a constant

over time suggesting a parallel shift in the drift curve for market shocks. Second eigen component shows a butterfly effect. This suggest a change in convexity of the forward drift curve. First eigen component tend to move in opposite direction for the shorter maturities but it tends to move in the same direction with the other two components as the maturity increases.

4.1.2 Eigen component analysis for on the money bucket

Let's take look at the eigen components for on the money bucket. Graph of those eigen components is shown below.

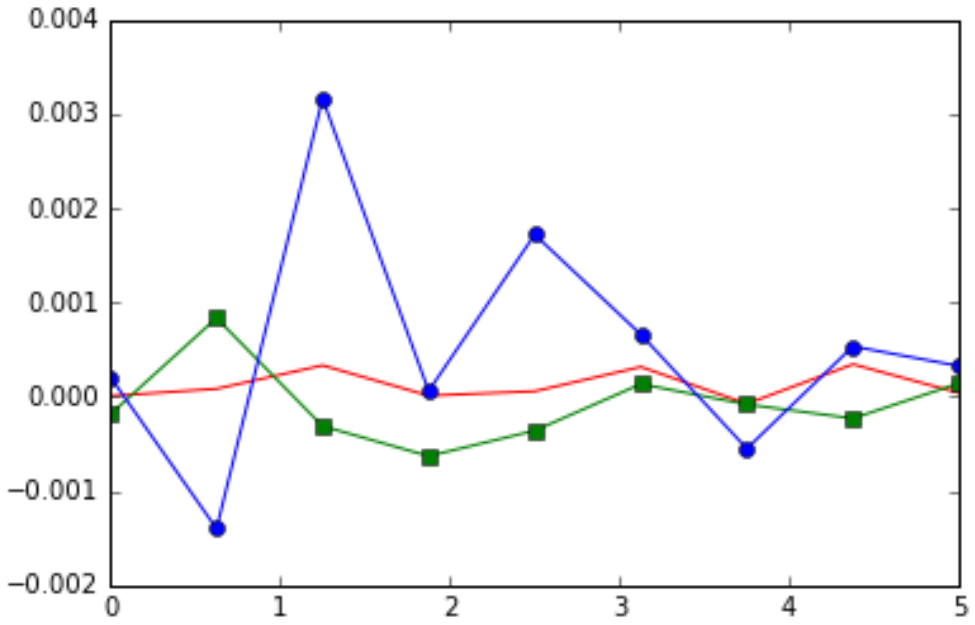

Figure 4.12: Eigen modes for on the money bucket

Just as in out of the money case, third eigen component represented by the solid line is very close to being a constant. Butterfly shape of the second component is not apparent for the second component. First eigen component moves opposite to the other two for shorter maturities but tends to move on the same direction as other two for larger maturities.

4.1.3 Eigen component analysis for in the money bucket

Let's take look at the eigen components for in the money bucket. Eigen plots are shown as below.

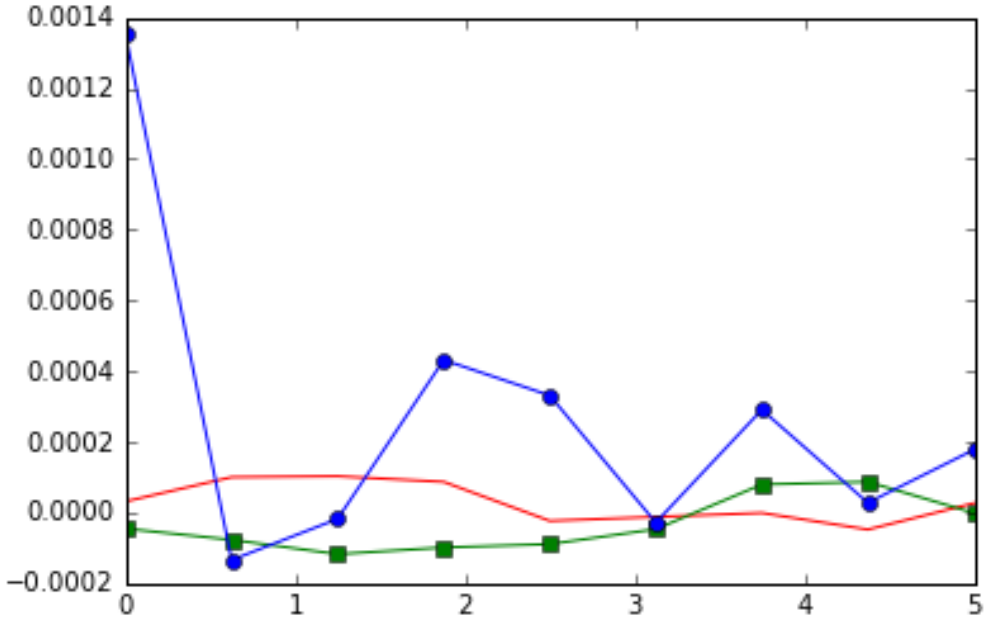

Figure 4.13: Eigen modes for in the money bucket

As we observed for out of the money and on the money buckets, third eigen mode shows a constant movement. Butterfly effect was not very clear for the second eigen component shown by the line with squares. First eigen component shows a lower correlation with other two components for shorter maturities but again shows a higher correlation with other components for higher maturities. This can be consistently observed for all three moneyness buckets.

We can observe some important distinctions between the shapes of eigen components of multiplicative model compared to additive model. Third eigen component in the multiplicative model shows a constant movement across time. Constant move-

ment of the eigen modes of the additive model is given by the second component. Both models shows a butterfly effect in the third eigen component although it is not very apparent for the multiplicative model. First eigen component shows a lower correlation with other two components for shorter maturities and it shows a higher correlation with higher maturities in the multiplicative model. We observed the opposite for movement of the first eigen component in additive model. This concludes the discussion of multiplicative model under regular principal component analysis.

4.2 Eigen mode analysis under robust principal component analysis

We will analyze the eigen component behavior using robust principal component analysis in this section. We will consider the same three maturity buckets as before.

4.2.1 Eigen mode analysis under out of the money bucket

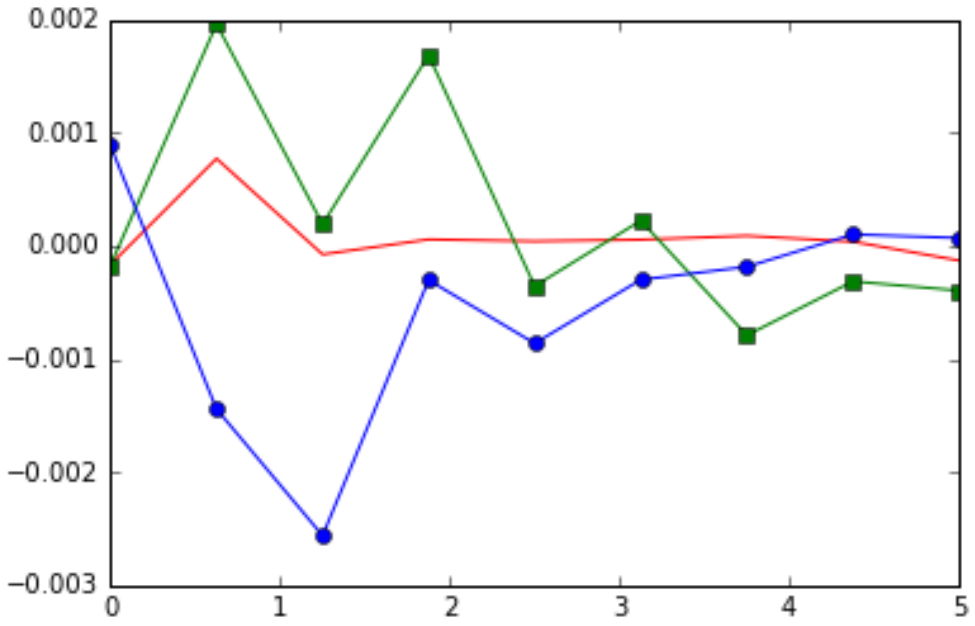

Figure 4.14: Eigen modes for in the money bucket using robust PCA

Note that the third eigen component given by the solid line shows a constant movement. Second eigen component, which is given by the line with squares, shows a butterfly shape. Which is consistent with what we have observed for out of the money bucket under the regular principal component analysis. First eigen component move in opposite direction to the first two components for shorter maturities while it is moving in the same direction of the other two components for larger maturities. We also noticed that the plots are very similar to those under the regular principal component analysis. This suggest that the missing data has a little effect on covariance matrix of data.

4.2.2 Eigen mode analysis for on the money bucket

We will analyze the eigen component behavior using the robust principal component analysis for on the money bucket in this subsection.

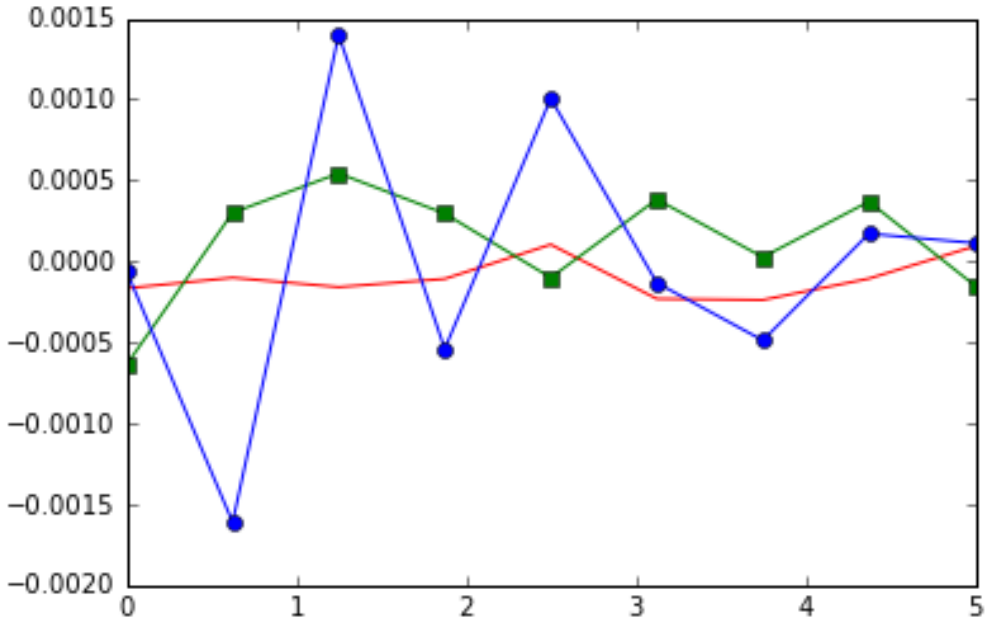

Figure 4.15: Eigen modes for on the money bucket using robust PCA

Third eigen component shows a constant movement for on the money bucket. Second eigen component is showing a butterfly shape just as we observed under the out of the money bucket. First eigen component shows a low correlation with the other two components for shorter maturities. It shows a higher correlation with the other two components for larger maturities.

4.2.3 Eigen mode analysis for in the money bucket

We focus on analyzing the eigen component behavior for in the money bucket in this subsection.

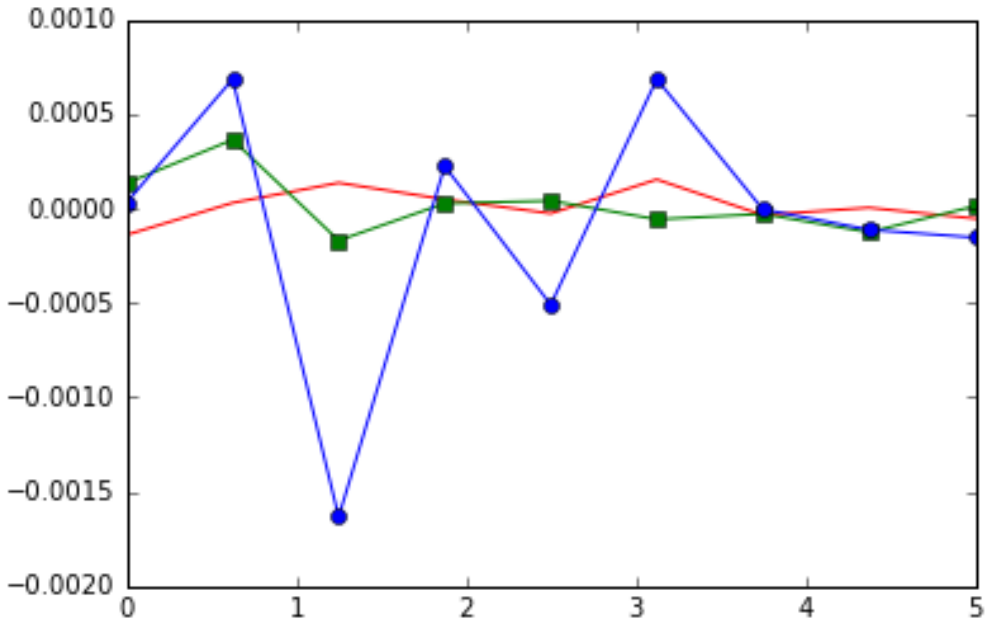

Figure 4.16: Eigen modes for in the money bucket using robust PCA

Just as in the previous two moneyness buckets, third eigen component shows a constant movement. Second eigen component which is given by the line with squares shows a butterfly shape over time. First eigen component given by the line with circles shows a higher degree of correlation to the second eigen component over time.

4.2.4 Overview of robust principal component analysis

We analyzed the shapes of eigen components under robust principal component analysis for three maturity buckets. We noticed that the third eigen component shows parallel shift in the drift curve for all buckets. Which is consistent with what we observed under regular principal component analysis. Similarly, the second eigen component shows a butterfly effect for all buckets under consideration. This is also consistent with what we have observed for the third eigen mode under regular principal component analysis. First eigen component consistently shows a lower correlation to the other two modes for lower maturities while correlation tend to increase for larger maturities. Overall behavior of three eigen components seems to be consistent with regular principal component analysis. We analyzed the shapes of eigen components for both additive and multiplicative model under two methods: principal component analysis and robust principal component analysis. With this, we concludes our investigation of eigen components.

4.3 Karhunen-Loeve (KL) transformation

We introduced KL transformation under additive model. Cont and Fonseca (2006) applied KL transformation to the difference matrix of implied volatility. We will apply the same technique for our data matrix under the multiplicative model. Cont and Fonseca (2006) modeled the eigen modes as a surface using equation 21 in their paper. Similar eigen surface for multiplicative model for is given by the following surface plot.

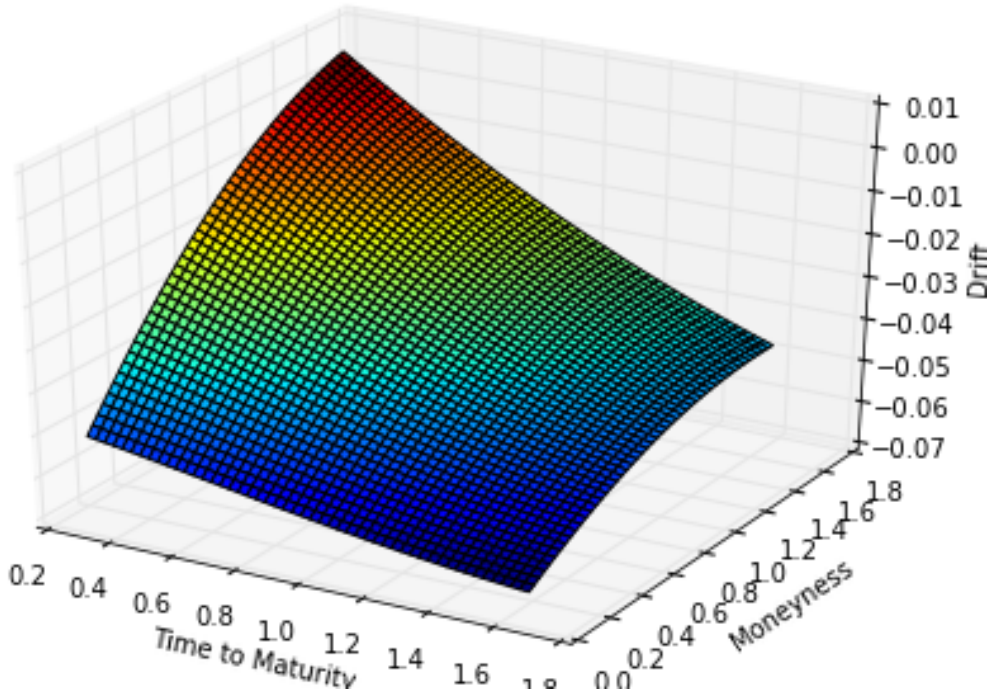

Figure 4.17: Eigen surface for forward drift process under multiplicative model

4.4 Simulation of forward drift curve for multiplicative model

We will demonstrate the simulation of the forward drift curve under the multiplicative model. Initial forward vector $f_0(T)$ is the same as for the additive model. Let's recall

$f_0(T) = [0.020058, 0.010608, 0.001523, 0.000265, 0.001108, -0.010265, 0.000115, -0.000221, 0.001095, -0.0002112, 0.000431, -0.000220, 0.000332]$

Let's recall the simulation function for multiplicative model.We model the dynamics by

$$f_t(u) = f_0(T) + \int_t^T \alpha_t(u)du + \sum_{n=1}^{m} \int_0^t \beta_u^n(T)du \tag{4.50}$$

where $\int_t^T \alpha_t(u)du$ as given in the theorem 4. Here we simulate the forward curve for

252 days. Also it's worth noticing that we only retain three Brownian factors since over 93 percent of the total variance is explained by first three eigen vectors. We will discuss how to estimate the volatility function in next subsections.

4.4.1 Estimation of volatility functions

Note that equation (4.35) involves σ_0 as well as $\beta_u^n(T)$. For the sake of simplicity we let $\sigma_0 = 1$. We will estimate $\beta_u^n(T)$ values using eigen components. Third eigen component shows a constant movement over three maturity buckets. Therefore, we estimate third eigen component by average of third component across three buckets. First and second eigen components does not appear to be fit into a simple deterministic function. But just as we saw under the additive model, those components seem to reflect mean reversion. Therefore, we estimate the first and the second eigen components by mean across given three buckets. Calculated volatility functions are given in the following table.

Table 4.4: Estimation of volatility functions for multiplicative model

Eigen mode	Variance
$\beta_u^1(T)$	-0.00091
$\beta_u^2(T)$	0.00073
$\beta_u^3(T)$	-0.000127

Simulation of the forward drift curve is carried out using the volatility functions given in table 4.4 and $\sigma_0 = 1$. Simulation function is given by the equation (4.32). Simulation of 100 paths are shown in the plot below.

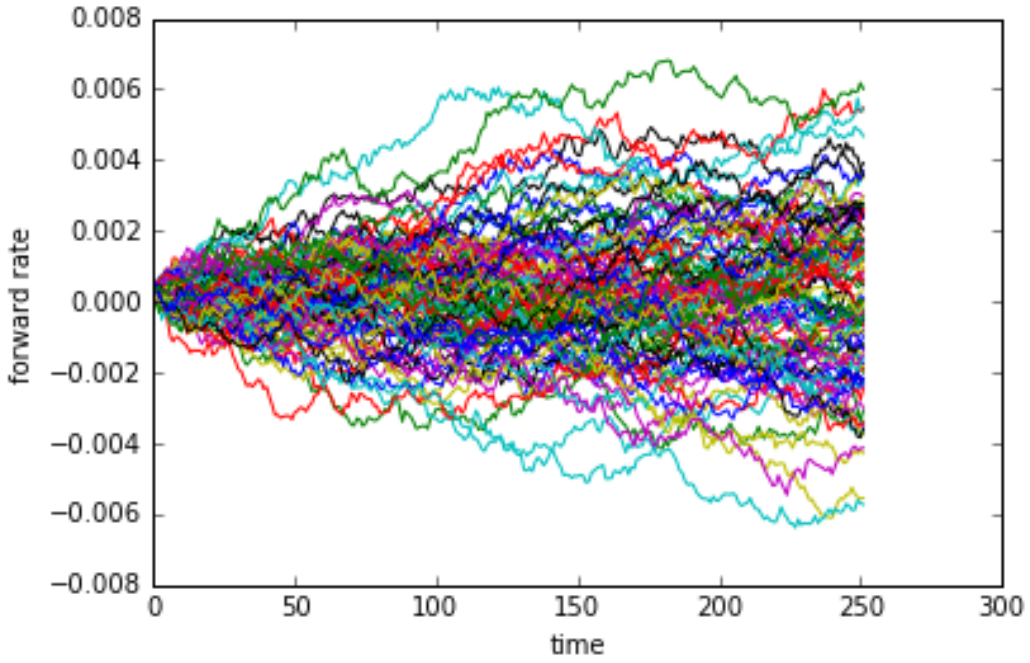

Figure 4.18: Forward drift simulation

Now we will discuss how to estimate the optimal stopping time for the multiplicative model using the forward drift. Let's recall the optimal stopping time τ^* under the multiplicative model is given by theorem 6.

$$\tau^* = \inf\{t \leq s \leq \tau : \int_s^T f_s(u)du \leq 0\}.$$

Just as in drift simulation for the additive model, we estimate the forward drift curve $f_t(u)$ by taking the average path of 100 simulated paths from the above simulation.

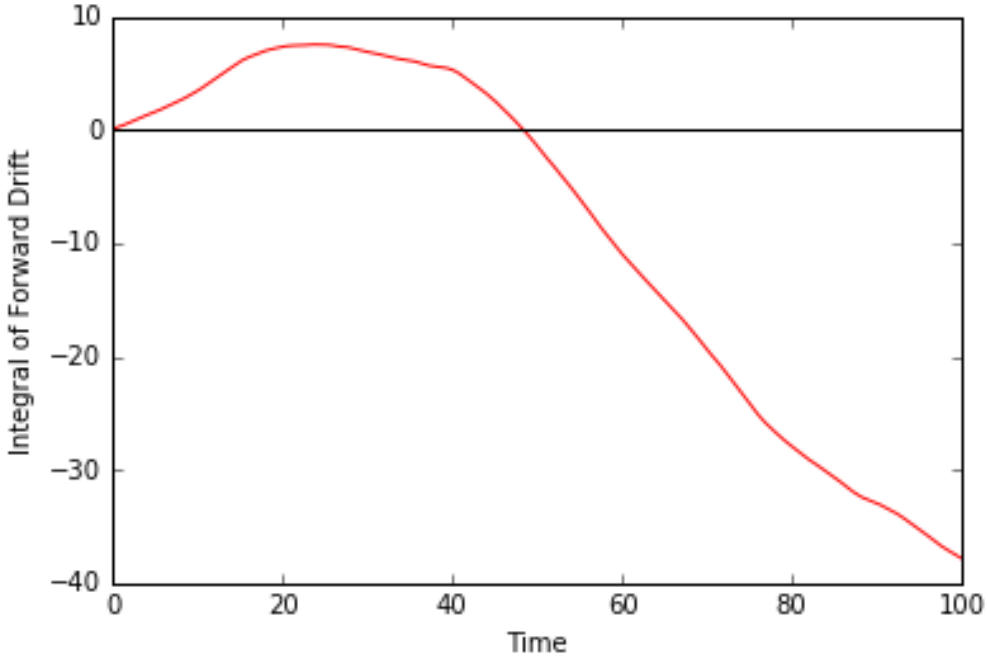

Figure 4.19: Integral of forward drift and stopping time

Our numerical simulation of the forward drift integral suggests that time index $s = 0$ is the first time $\int_s^T f_u(s)du \leq 0$. Therefore, the optimal stopping time is the index $s = 0$.

Here we did analyze the eigen modes for three maturity buckets for the multiplicative model. We employed traditional principal component analysis, robust principal component analysis since our data contained missing values. Further we used KL transformation to construct eigen surface. We observed that the third eigen component shows a parallel shift in the forward drift curve. Second eigen component shows a butterfly effect. First eigen component shows a low correlation with other two eigen modes for shorter maturities.

CHAPTER 5: CONCLUSION AND FUTURE WORK

In this thesis, we proposed a new method to price American type derivatives using forward modeling approach. We introduced a new value function V_t as an alternative solution to the traditional optimal stopping problem. Then we introduced a new stopping criteria and the new stopping time associated with it. Then we carried out numerical investigation of eigen components according to three methods: principal component analysis, robust principal component analysis and Karhunen-Loeve transformation.

Historical studies on yield curve suggests that first eigen component shows a parallel shift in the yield curve. Similar behavior can be seen for volatility surface analysis as well. We analyzed the forward drift curve under two models: additive model and multiplicative model. The additive model yields that the second eigen component shows a parallel shift in the drift surface. Our multiplicative model analysis suggests that the third eigen component shows a parallel shift. Similarly Skiadopoulos, Hodges and Clewlow (1999) observed that the second eigen component in the yield curve shows a bend or a twist. Cont and Fonseca (2006) found similar behavior for the second eigen component by studying a cross section of volatility surface. They also noticed that second eigen component shows a higher correlation to moneyness. Our analysis of drift surface shows that under the both additive and multiplicative models, there is a correlation between the first eigen component and the other two when time to maturity varies. Cont and Fonseca (2006) found that the butterfly effect is apparent for third eigen component for implied volatility surface. Further-

more, we observed that the second eigen component shows a butterfly effect under both additive model and multiplicative model.

One direction of improvement of this work is to estimate the parameters of the surface given by KL transformation and model the surface in dynamic manner. Another area of development is to estimate eigen modes as a time series model as in Cont and Fonseca (2006).

Bibliography

[1] Steven E. Shreve. *Stochastic Calculus for Finance II Continuous-Time Models, 2nd Edition, Springer-Verlag.* 2000.

[2] Peskir & Shiryaev. *Optimal Stopping and Free- Boundary Problems. Birkhauser.* 2006.

[3] I. Karatzas, S. Shreve. *Brownian Motion and Stochastic Calculus, 2nd Edition, Springer-Verlag.. Spriner Finance.* 2000.

[4] M. Schweizer, J. Wissel. *Term Structures Of Implied Volatilities: Absence Of Arbitrage and Existence Results, Mathmetical Finance.* 2008.

[5] Paul Wilmott. *Introduces Quantitative Finance, 2nd Edition.john Wiley & Sons.* 2007.

[6] D. Heath, R. Jarrow, A. Morton. *Contingent Claim Valuation with a Radom Evlution of Interest Rates, The Review of Future Markets.* 1990.

[7] D. Heath, R. Jarrow, A. Morton *Bond Pricing and Term Structure of Interest Rate: a new methodology,Econometrica* 1992.

[8] Bruno Dupire. *Pricing with a Smile.Bloomberg.* 1994.

[9] R. Carmona, S. Nadtochiy. *Local Volatility Dynamic Models, Finance & Stochastic.* 2009.

[10] S.Dayanik, I. Karatzas. *On the Optimal Stopping Problem and Their Applications, Stochastic Processes and their Application.* 2003.

[11] M. Schweizer, J. Wissel *Term Structures of Implied Volatilities:Absence of Arbitrage and Existence Results , Mathematical Finance.* 2008.

[12] R. Carmona, *HJM: A Unified Approach to Dynamic Models for Fixed Income, Credit and Equity Markets.* 2009.

[13] Darrell Duffie *A Yield-Factor Model of Interest Rates , Mathematical Finance.* 1996.

[14] P. Schonbucher, *A Market Model for Stochastic Implied Volatility.* 1998.

[15] D.Brigo & F.Mercurio *Interest rate Models-Theory and Practice, 2nd Edition, Springer Finance.* 2007.

[16] O.Vasicek *An Equilibrium Characterization Of The Term Structure.* 1977.

[17] R. Carmona, Y.Ma, S.Nadtochiy *Simulation of Implied Volatility Surfaces via Tangent Levy models.* 2015.

[18] Y.Ma *Implied Volatility Surface Simulation with Tangent Levy Models.* 2014.

[19] R. Cont, J.Da Fonseca *Dynamics of implied volatility surfaces.* 2006.

[20] L.E.O.Svensson *Estimating and interpreting forward interest rates.* 1994.

[21] G.Skiadopoulos,S.Hodges,L.Clewlow *Dynamics of the S&P 500 implied volatility surfaces,Review of derivatives research* 1999.

[22] H.Abidi,L.Williams *Principal component analysis,WIRES computational statistics.* 2010.

[23] E.Candes,X.Li,Y.Ma,J.Wright *Robust principal component analysis?,Microsoft research Asia,Beijing,China* 2009.

[24] US Department of the Treasury, Resource Center, Daily Treasury Yield Curve Rates. https://www.treasury.gov/resource-center/data-chart-center/interest-rates/Pages/TextView.aspx?data=yield, 2017.

[25] dubourg/python-randomfields. https://github.com/dubourg/python-randomfields/blob/master/2Dkarhunenloevesimulationexample.py, 2013.

[26] Principal Component Pursuit in Python https://github.com/dfm/pcp, 2015.

[27] A.T.Koken *Implementation of the Heath-Jarrow-Morton model on the Turkish government zero-coupon bonds* , 2013.

[28] Option Matrix http://optionmatrix.com, 2017.

[29] Wrds database https://wrds-web.wharton.upenn.edu/wrds, 2017.

[30] Crisp database http://www.crsp.com, 2017.

[31] Anaconda continuum analytics https://www.continuum.io, 2017.